University of Stavanger

Faculty of Science and Technology

MASTER'S THESIS

Study program/ Specialization: **Mathematics and Physics**	Spring semester, 20.15..... Open access
Writer: **Pattarini Giorgio**	.... (Writer's signature)
Faculty supervisor: **Prof. Per Amund Amundsen, UiS** External supervisor(s): //	
Thesis title: **Some models for the magnetization of the drilling mud**	
Credits (ECTS): **60**	
Key words: MWD, directional drilling, directional survey, ellipsoid, effective, langevin, paramagnetism, Stavanger, Physics, mixing, statistical, DRM, paleomagnetism, suspension, alignment, mud, drilling mud, magnetic contamination, error	Pages: ......V + 62.............. + enclosure: .... Stavanger, **15 June 2015................** Date/year

Some models for the magnetization of the drilling mud

Giorgio Pattarini

June 2015

MASTER THESIS

University of Stavanger

Institutt for matematikk og naturvitskap

Universitet i Stavanger, Norway

Supervisor: Per Amund Amundsen

Preface

This is a the final report of the research work carried as duty to complete the Master thesis in Physics at the University of Stavanger in the 2014 Fall and 2015 Spring semesters. The subject of the research is a technical issue from the Oil industry, that has been explored with the methods of Physics,

Stavanger, Norway June 15, 2015

Giorgio Pattarini

Acknowledgment

I would like to thank the following persons for their help during the master: at first the supervisor Prof. Per Amund Amundsen, that identified as physically interesting the subject of the magnetization of a suspension, and provided a great load of ideas and methods to tackle it.

Furthermore, many other professors have helped with notions and suggestions:

- Arild Saasen, professor at UiS, that provided continuous support on all details regarding the drilling mud, together with background and industrial experience on the mud magnetization issue;
- Helge Hodne, professor at UiS, who suggested to use the Paleomagnetic studies as reference;
- Udo Zimmermann, professor at UiS, for a fruitful discussion on natural magnetic rocks;
- Ingve Simonsen, professor at NTNU, for a short but useful discussion on thermodynamics;

I must also thank Martin Tangeraas from Stavanger and Prof. Sigbjørn Hervik of UiS, who made me to enrol at the Master two years ago.

Most of the support during the master has come from my girlfriend Elena, that I thanks with all my hearth.

The University costs have been supported by the Norwegian taxpayers and by the Oil revenues, that I sincerely hope to ricompensate.

Giorgio Pattarini

13 June 2015

Short Summary

The problem that a magnetic drilling mud cause to the accuracy of the directional drilling technology is outlined. The purpose of the work is identified in the theoretical modelling of the magnetic response of the magnetic mud, a fluid that is contaminated with small amounts of magnetic materials. The theory of mixing magnetic materials is reviewed, practical results are derived in detail and discussed. The classic model of an ellipsoid, instrumental for the calculations, is presented in detail. Are then defined and developed the models for suspended particles under the combined effect of a magnetic field and Brownian motion; the predictions are compared to the available experimental data.

Contents

1

Introduction

"ANDREA: I would like to become a physicist like you, Galileo.

GALILEO: Surely I agree with you, since there is a huge amount of problems still to solve in our field."

– Bertold Brecht, *Life of Galileo*

1.1 Background

Between the many human activities, the hunt for energy has a prominent role; a part of the modern energy needs is covered by natural fossil Oil and Gas, that have to be extracted from underground deposit through deep and expensive wells.

Oil wells have been traditionally vertical, but in recent times it has been started to drill deviated and horizontal wells, in the continuous race to get more oil while the reserves become less accessible. Deviated wells are extensively used in Offshore field developments, in order to exploit a wide area with a single platform; horizontal wells are drilled for the production of shale gas, as a long section of well is needed inside the typically shallow and horizontal reservoir.

Outside the Oil industry, drilling horizontal bores is used to create buried channels that can house cables and pipes, as an alternative of digging a trench, lay the cable and cover it again.

The technology has been called *directional drilling*, and present a set of new challenges with respect to the normal boring of a vertical, straight hole. The first challenge is to convince the drilling bit to change direction; isn't easy but many techniques have been effectively applied, so that the drilling direction can be changed at will.

However, this control of the steering is not accurate, depending on many factors that could alter the given direction and eventually lead to miss the planned target. As a result a survey system is needed, complementary to the physical steering system, able to detect and estimate where and in what direction the bit is going, in order to implement the indispensable corrections to stay on track.

This latter issue has generate a subject of its own, often called *steering survey*, and a lot of techniques have been developed to gauge the position and the direction of the drilling bit; a prominent role is taken by the Measurement While Drilling (MWD) systems, consisting on a set of sensors, mounted right after the drilling bit, that can communicate their readings from the bottom of the well to the surface, enabling the rig crew to know the actual direction almost in real time.

Down inside the Earth's crust, is not possible to rely on the GPS or look at the stars to get the direction, so the survey must rely on directional signals that are detectable also under the surface, like the gravitational field and Earth's magnetic field[1]. Then, the typical set of sensors consists of an accelerometer, that detect the direction of the gravitational acceleration and hence the vertical inclination of the assembly, and a directional magnetometer, that sense the direction of the magnetic North.

The attention is then zoomed on the detection of the magnetic field, and a detailed view will reveal that the determination of the North is not simple at all, and is prone to many systematic errors and unavoidable uncertainties, that degrade the accuracy of the direction survey impairing the performances of the Directional Drilling.

The errors can come from different sources: the sensor can be faulty; the drill bit and the drill string are made of steel and can be magnetized, deflecting the local field; Earth's field can naturally vary over space and time; and so on. All the main error contributions must be taken into account, to implement the necessary correction and assess the effective uncertainty. Between those sources, a special place is taken by the magnetic error induced by the drilling mud, that is the subject of this thesis work.

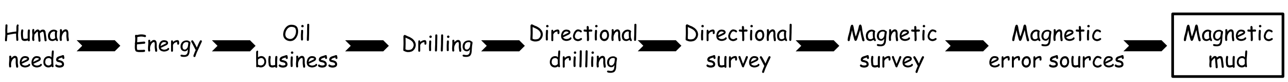

Figure 1.1: A summary on how the magnetic mud fits in the big picture. A similar summary, for the magnetic mud modelling, is represented in figure 4.1 in the Conclusions. [100]

The problem of the magnetic mud

The drilling mud is the fluid that is pumped down the well to lubricate the drill bit and remove the cuttings, and it can constitute an important source of error in the magnetic survey. The mud is usually magnetically inert, but during normal operations it could become contaminated with magnetic particles like steel wear filings, and thus acquire strong magnetic properties.

[1]Other interesting signals that could be available at depth, like neutrinos or gravitational waves, are not easy to detect.

A magnetic drilling mud can shield or deflect the Earth's magnetic field, affecting the readings of the sensors that are surrounded by the mud. This issue is known since many years and it is credited to cause serious problems in specific conditions; however, a clear interpretation of the phenomenon, along with a technique to quantify the error induced, has not been developed yet. To understand the magnetic properties that the mud

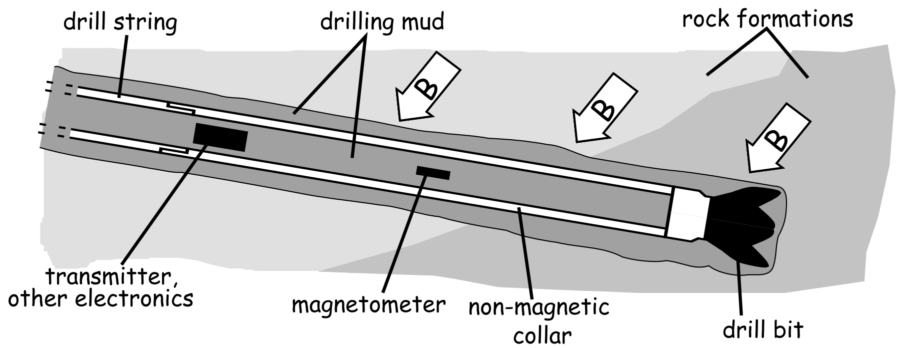

Figure 1.2: A sketch of the bottom hole assembly in operation. All the elements illustrated can bring significant error on the measurement of the Earth's magnetic field **B**. Now, the attention is all on the drilling mud contribution. [105]

acquires when contaminated, have been carried experiments and proposed interpretations. The Directional Drilling application was the original source of the challenge, but in order to understand and model how the magnetization of the mud arises, the sharp tools of physics are needed.

The modelling of the drilling mud can rely essentially on the methods developed for electromagnetism, statistical physics and mathematical analysis. However, the magnetization of the mud has many analogues in nature and in technology, thus the modelling process can benefit from the contributions coming from different fields of science. Fields and application that can provide relevant insight include the theory if dielectrics, the science of paleomagnetism, even astrophysics and the technology of composite materials.

Literature survey

There exist an official guideline for the evaluation and correction of errors in the directional survey of deviated wells, issued by the ISCWSA committee [29], but the magnetic mud contribution is not included yet, and is being currently discussed [21, 36]. The detrimental effects of the magnetic mud had been identified several years ago, and early studies are presented in the references [18, 17, 19], that also model the importance of the effect with respect to the well orientation. More geometric aspects of the field deviation are addressed in [20, 31, 32].

The properties of real drilling mud have been measured [18, 28, 30], identifying the root cause of the magnetic properties in small amounts of magnetic contaminant particles. Some experiment have been carried, [26, 30, 35], measuring the magnetic shielding effect of muds prepared mixing an inert base with magnetic particles.

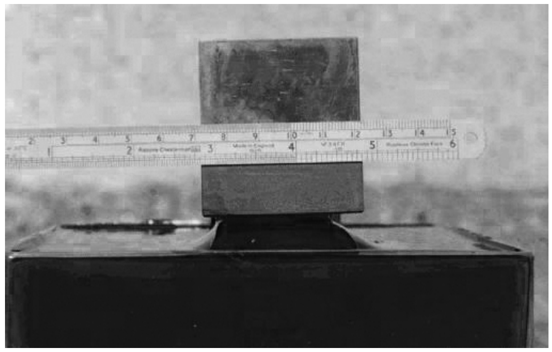

Figure 1.3: The empirical evidence: real drilling mud in a bucket is attracted and lifted by a strong magnet. Image from [28]. [14]

The physical modelling of the mud from first principles is approached in some publications, [25, 34, 33] and some Thesis works [23, 22, 27].

The problem of the magnetic mud is very similar to others encountered in science, like the effective polarization of a dielectric [3, §8], the Langevin theory of paramagnetism [2, §28] the Detrital Remanent Magnetization in paleomagnetism [7, 77].

What remains to be done?

The origin of the magnetic properties of the mud had been identified in small quantities of strongly magnetic particles suspended in the fluid, but the physics of such a suspension remains unclear. Models for magnetic suspensions exists, but have not been completed or properly adapted. Some experimental result are puzzling and need completely new models to be explained. All those issues are to be addressed, in order to set up reliable system that could be used to estimate the magnetic properties of the mud, given the amount and properties of the contaminants.

More experimental work should be needed also, specially to measure size, shape and composition of the contaminating magnetic particles. Experience on the field is needed to track the origin of such contaminants, and understand what procedures can reduce the problem without being too expensive.

Then, the effect on the magnetic measurements need to be carefully evaluated, and a simple error model must be selected, to be implemented in the whole directional survey system. Contaminant concentration limits should be settled, together with a way to assess such limits in field operations; the procedures needed to keep the contamination under control must be checked or restated where needed.

1.2 Objectives

This Master project is focused on the physical modelling of the drilling mud, as it was identified to be the critical link in the chain, as well as the most attractive issue from the scientific point of view. The starting point had already been settled, with an empirical benchmark and fundamental theoretical insights. The general purpose of this work is to improve the theoretical understanding on the magnetization of the mud; in detail, the job had been divided into six different objectives:

1. Review, assess and improve the models already proposed;
2. Research in the literature for existing models and methods applicable to the drilling mud;
3. Identify the core physics of the mud magnetization, defining the theoretical framework;
4. Explain the peculiar behaviour seen in the experiments;
5. Provide practical formulas and estimates;
6. Provide an accountable derivation of the results.

Limitations

This study is limited to the theoretical modelling of the mud, and do not include the geometric and directional variables needed to evaluate the error induced on the directional survey. Most of the space is filled with calculations and estimates, leaving few room for extensive introductions and broad overviews of all the arguments touched.

The experimental data are limited, as always, so many variables in the models cannot be quantified accurately.

Several approximations are made in the course of the work, many of which could be questioned; the modelling has been carried with a classical, macroscopic and mechanical style, thus neglecting a number of phenomena, like those arising from chemical, colloidal and quantistic properties. This simplification has been made for the lack of informations on the microscopical processes going on in the mud, for the personal limitations of the researcher, and for the daunting amount of deep complications that will derive when including all the details imaginable[2].

1.3 Outline of the report

In the report, the models for the magnetization of the mud are derived, with a prominent part taken by modelling a suspension of magnetic particles, see figure 1.4.

[2] A models to be useful needs to be simple, but there always the risk of excluding something crucial!

For those who have no time to read the whole thesis, the essential results are listed in the section 4.2.

In the chapter 2 are at first briefly defined the needed elements of magnetism: is then presented the theory for the effective properties of a mixture of two different substances, typically one medium and the suspended solids, when they are not allowed to move. This subject is commonly presented in electrostatic, and is here adapted for the magnetic case. The main result of the theory are the mixing formulas, that are evaluated for some examples.

The following chapter 3 is the key one, with the model of a suspension of magnetic particles, free to move,

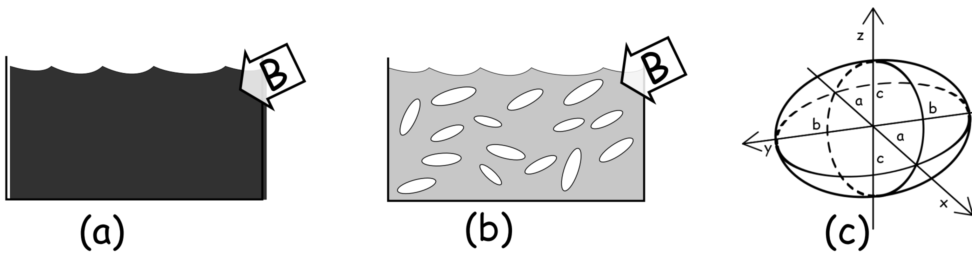

Figure 1.4: The main subjects of this thesis: (a) the real drilling mud, subject to the Earth's magnetic field **B**; (b) the model of the drilling mud, a suspension of magnetic particles oriented with **B** (c) the model of the shape of the suspended particles, an ellipsoid [114]

subject to the magnetic forces that have to fight against the disordering Brownian motion. Calculation of the resulting magnetization is carried for dipoles, reproducing Langevin's theory, and for ellipsoidal paramagnetic particles. Limiting cases and quantitative estimates are evaluated.
In the last chapter 4 the main results are briefly reviewed, and are indicated some suggestion for future work.

An illustration of the main features of the drilling mud is in appendix A; is very short and could be read before the other chapters, to get familiar with the object of the report. In the following one B are collected the representative numerical values used for the estimations.

In the bulky appendix C there is "the Ellipsoid in all its glorious details", where are reported the calculations and the results for the classic model of an ellipsoid immersed in a uniform field. The magnetic particles considered in chapters 2, 3 are always modelled as ellipsoid, using the results from this appendix.
The thesis is a bit long, but there are a many illustrations. Good reading!

⋈

2

The effective susceptibility of a mixture

2.1 Definitions and units for the magnetic field

"To proceed further we must establish the physical dimensions of these vectors and ***agree*** *on the units in which they are to be measured "*

– J. A. Stratton, after presenting Maxwell equations

The definitions and units of measure in magnetostatic are a bit tricky, and is useful to outline the main quantities involved. It is also mandatory, as the quote suggest, to state what units of measure are used. Since the topic of this thesis stem from an engineering application, will try to use units from the International System (SI) [119]. In the following are outlined the salient quantities of magnetostatic; detailed description can be found in most texts of Electromagnetism [1, 3, 9, 33], although sometimes they still don't agree about notations or units. It is useful to remark that the present work will encompass only static or quasi-static conditions and macroscopic or quasi-macroscopic ones; although it is founded on magnetism, it will not need any knowledge of what magnetism really is, or where it comes from. A careful use of the following definitions, joined with Laplace equation alone (Maxwell's ones will stay hidden!) is all what is needed to build a classical theory for the magnetization of our drilling mud.

The magnetic field **B**, or magnetic flux density, is expressed in Tesla $[\mathrm{T}]$ or micro Tesla $[\mu\mathrm{T}]$. In classical vacuum this flux density is related to the 'field strength' **H** by the relation

$$\mathbf{B} = \mu_0 \mathbf{H}$$

Where **H** is measured in Henry or Ampere per metre $[\mathrm{A\,m^{-1}}]$ and the vacuum permeability $\mu_0 = 4\pi \cdot 10^{-7}$ is a scalar (vacuum supposed to be isotropic!) with the adjusting dimensions $[\mathrm{T\,m\,A^{-1}}]$. When a material is present, it can affect the field with a property $\mathbf{M}$ called magnetization:

$$\mathbf{B} = \mu_0(\mathbf{H} + \mathbf{M})$$

For many common materials within a reasonable range of applied field, the magnetization is induced by the field and is linear on it: $\mathbf{M} = \chi\mathbf{H}$. Those material are called paramagnetic or diamagnetic, depending on the sign of the proportionality constant χ. In general, χ is a tensor, since the induced magnetization can depend on the direction of the imposed field, that sounds reasonable for crystalline solids. It is anyway very common, and usually a good approximation, to consider χ a scalar, stating that the material is isotropic. Exploring the effect of the crystalline anisotropy could be of great interest and has been included in the 'Recommendation for future work' wish list. Forgetting all that, let's introduce the (scalar) permeability μ of the material and the previous equation can be rewritten:

$$\mathbf{B} = \mu\mathbf{H} = \mu_0(1 + \chi)\mathbf{H} \tag{2.1}$$

Note that $\chi = (\mu - \mu_0)/\mu_0$ is the volumetric susceptibility of the material, dimensionless; to add a bit of complication, is often measured and reported in term of the mass, thus needing a correction with the density ρ: [1] $\chi_{mass} = \chi/\rho$.

Materials like iron and magnetite are called ferromagnetic, they don't fit well with the simple linear relation and can hold a permanent magnetization $\mathbf{M}$ even in absence of the external field. And there are of course a great number of other materials with strange names, that exhibit the weirdest functional relations with the applied field, but won't be considered here[2]. Often the term magnetization is used to indicate the remanence, $\mathbf{R}$ specially to measure the strength of permanent magnets, but this time is expressed in Tesla, $\mathbf{R} = \mu_0\mathbf{M}$.

For the present application also the energy density stored in the magnetic field can be easily defined:[3]

$$U_m = \frac{1}{2}\mathbf{H} \cdot \mathbf{B} \tag{2.2}$$

This energy density is, incredibly, already set in the SI units of Joules per cubic metre $[\mathrm{J/m^3}]$.

[1] And the density weight could be expressed in pounds, grams, ounces, MeV or whatever, so tabulated values must be carefully checked.

[2] Well, the entire work of this thesis consists on studying the weird reaction of the drilling mud on the applied field, thus falling in this last category; but its component are always considered to be nicely Paramagnetic, and sometimes ideally ferromagnetic

[3] A proper definition of the magnetic energy can be very tricky [8, p.21, p.337] but in this work there is no need to worry since a) the field is external and constant in time, b) all the components of the system were already there, and c) all the interest is only on the variations of the energy.

2.2 Mixing Formulas

As was illustrated before, the drilling mud is a rich blend of several different substances. If the magnetic response of the single ingredients is known, is it possible to infer the properties of the mixture? This issue is quite old and wide considering also the mathematical equivalence between magnetostatic and electrostatic. The most ancient and simple mixing formula, the weighted average, often called Wiedemann's law [20], [117, p.349] when applied to the magnetic susceptibility, could be not enough to describe many situations of interest.

Essentially, in a static or semi-static environment, all the following quantities have an equivalent approach: magnetic Permeability, Dielectric constant, Refraction index, electric and heat Conductivity; almost wherever a Laplace equation is in place.

Figure 2.1: Some of the many fathers of the mixing formula [98]

Since there are different fields of science involved, the fundamental *Mixing Formula* that solve the current problem has different versions and names, in honour of those that have refined it for every new application: the oldest version is the Clausius-Mossotti [37, 38] dating back to 1850, then came Maxwell-Garnett, Lorenz-Lorentz, Railegh, Bruggeman, Polder-van Santen, Onsager, and probably others. [4]

The essential formula can be derived, among other ways, by considering spheres suspended in a medium of different permittivity. The field inside a sphere can be sorted out from one of the listed electromagnetic books, [3, §9], or better evaluated as a special case from the appendix C, using equations (C.10), (C.12) with parameters from the table C.1. The two ways should match and provide as result for the field $\mathbf{B}_-$ inside the sphere:

$$\mathbf{B}_- = \mu_1(\mathbf{H_0} + \mathbf{M}) = \mu_1(\mathbf{H_0} + \mathbf{L}\mathbf{H_0}) = \mu_1 \mathbf{H_0} \frac{3\mu_2}{2\mu_2 + \mu_1}$$

Where μ_1 is the permittivity of the sphere and μ_2 that of the medium. Defining now the effective large-scale permittivity μ_{eff} of the mixture with the equation

$$\overline{\mathbf{B}} = \mu_{eff} \overline{\mathbf{H}} \tag{2.3}$$

Where the bars stands for spatial average. Said δ the volume fraction of the spheres, the effective susceptibility

[4] Even the famous Einstein's formula on the viscosity of a suspension of rigid spheres can be seen as a special case of mixing.

results as:

$$\mu_{eff} = \frac{\overline{\mathbf{B}}}{\overline{\mathbf{H_0}}} = \delta \frac{\mathbf{B}_-}{\mathbf{H_0}} + (1-\delta)\frac{\mathbf{B}_+}{\mathbf{H_0}} = \delta \frac{\mu_1 \mathbf{H_0} \frac{3\mu_2}{2\mu_2+\mu_1}}{\mathbf{H_0}} + (1-\delta)\mu_2$$
$$= \mu_2 \Big(1 + \frac{3\delta(\mu_1 - \mu_2)}{\mu_1 + 2\mu_2 - \delta(\mu_1 - \mu_2)} \Big) \quad (2.4)$$

This is the Maxwell-Garnett formula for magnetism, that gives the susceptibility of a dilute suspension of spherical particles; it is the first useful result for the determination of the susceptibility of the drilling mud, knowing properties and concentration of its components.(Maybe is the first time this formula is applied to drilling mud, but it is not brand new nor original: this form dates back to 1904 [40]).

Beware, the formula not exact: the particles must be spherical and well diluted, meaning non interacting; see [49] for a numerical comparison and a quantification of the error. It holds its age anyway very well, and could be applied with success, specially thanks to the upper and lower bounds set by the paper [46] for an arbitrary mixture. The diluted condition is not so strict, allowing a good match up to several percentage point, and even over the whole composition range if also the 'flipped' version of the formula is used, when what was the medium is modelled as spherical inclusions as in figure 2.2.

Thanks to the many scientists that have worked on the mixing problem, there are several ways to improve this formula, see for example [45, 47, 48, 10, 50, 51, 52]. For the present purpose this approximation is considered enough, and the formula will be extended in the next sections only in the case of ellipsoidal suspended particles.
as final approximation, let's take the susceptibility χ and the concentration δ both small ($\chi \simeq 10^{-5}$ for most

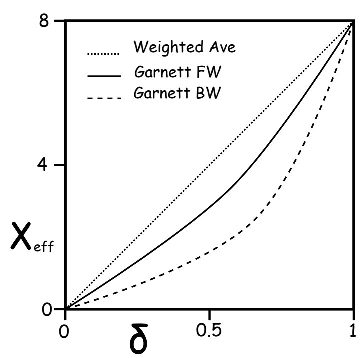

Figure 2.2: A plot of the effective susceptibility, from equation (2.5), compared with the linear Wiedemann law. The FW line is obtained with the inclusions having $\chi_1 = 8$ and the medium $\chi_2 = 0$ while in the BW line the roles are swapped. Note that the Garnett plot differ from the weighted average already for $\delta \ll 1$, since the χ in this example is not small. [40]

The equation 2.4, considering the medium with permeability close to the vacuum one, $\mu_2 = \mu_1$, can be cleanly expressed also in terms of volumetric susceptibility $\chi = (\mu_1 - \mu_0)/\mu_0$:

$$\chi_{eff} = \frac{\mu_e ff - \mu_0}{\mu_0} = \frac{3\,\delta\,\chi}{3 + \chi(1-\delta)} \quad (2.5)$$

This function is plotted in fig 2.2.

materials without iron); the amazing result is

$$\chi_{eff} = \delta\,\chi \tag{2.6}$$

That is, the result that would be obtained by the weighted average of Wiedemann's law, simply taking the volumetric weighted average of the susceptibilities. Whenever the ingredient added has no powerful paramagnetic properties, this last straightforward formula can be successfully applied.

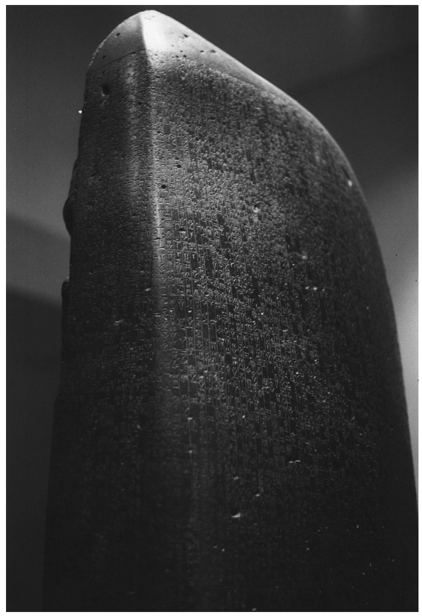

Figure 2.3: The ancient mother of all mixing formulas, the weighted average; here reported in the Hammurabi code stele, ca 1750 BC

2.3 A suspension of paramagnetic ellipsoids

The particles suspended inside the drilling mud have no reason to be spherical. The bentonite, one of the main gelling ingredients of the drilling mud, is composed of thin platelets. But the main reason to model the suspended particle as non-spherical is to try to understand the dynamical magnetizing behaviour observed by Amundsen et al.[25] and by Ding et al. [26]. In this first section is developed the static or equilibrium case, using the methods of the effective permittivity, while the trial of reproducing the dynamics is left to the following chapter.

The non-spherical particles are modelled as ellipsoid, since for this shape exist a clean analytical solution, that is described in detail in the Appendix A, from which the main results are taken. A light analytical approach impose also to restrict the general ellipsoid to a spheroid, meaning setting two of the axes equal. This restriction reduce the adherence with realistic cases, but is considered sufficient to capture the physics of the system.

2.3.1 Mixing for ellipsoids

Similarly to the mixing formulas, also the suspension of ellipsoids has a long story. It is chosen here to follow the line of Sihvola [10, 48], adapted for the special paramagnetic case. The first and simplest case to study is when all ellipsoids are aligned, like in figure 2.4 Let's take a large number of ellipsoidal particles, all with

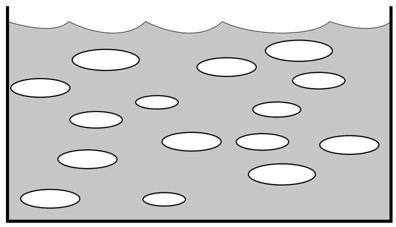

Figure 2.4: A fictitious suspension where all the particles are perfectly aligned, perfect ellipsoids and even with the same proportions. The mixture is manifestly non isotropic.[107]

same proportions and aligned all together; the size can vary. Let also the suspension be sufficiently diluted, so the nightmare of particle-particle interaction can be neglected. The Cartesian axes are set to correspond with those of the ellipsoids; in one of those Cartesian direction, say x, parallel to the a axis of the ellipsoids, the external field is H_x and the resulting field inside one of the ellipsoid is determined by the demagnetizing factor L_{11} as in equations (C.10), (C.12):

$$H_x^- = H_x^0 - L_{11}\frac{1}{\mu_0}P_{1x} = H_x^0 + N_a\frac{\chi_1-\chi_2}{\chi_1}\cdot\frac{1}{\mu_2}(\mu_2-\mu_0)H_x^0 = H_x^0(1-N_a\chi\frac{\chi_1-\chi_2}{\chi_1}) \simeq H_x^0\,(1-N_a\chi) \quad (2.7)$$

Where the last approximation has been made under the assumption that the permeability of the medium is the vacuum one μ_0 (as is often the case, as the base fluids of the mud possess very low susceptibility), and using the susceptibility instead of the permeability. This setup will be kept from now on, since allows much more compact expressions and all derived expressions could be re-tuned to the general case if needed.

The Garnett equation (2.5) can easily take the demagnetizing factors of the ellipsoid instead of those of the sphere, so the effective susceptibility in the x direction (identical to the a direction) results, with δ the small volumetric fraction of ellipsoids:

$$\chi_{eff\ a} = \frac{\delta\,\chi}{1+N_a\,\chi\,(1-\delta)} \quad (2.8)$$

The other components of the susceptibility can be obtained analogously, and the result is a non-scalar susceptibility, meaning the mixture has different properties in different directions, but still with diagonal form, thanks to the coordinates parallel to the axes of the ellipsoid:

$$\chi_{eff} = \begin{pmatrix} \chi_a & 0 & 0 \\ 0 & \chi_b & 0 \\ 0 & 0 & \chi_c \end{pmatrix} \quad (2.9)$$

A direct practical application of this model is for the susceptibility of deformed rocks, where the inclusions of different minerals have been smeared all parallel, giving rise to an anisotropic texture. In the drilling application a perfect alignment is unrealistic, and a more general approach is needed.

2.3.2 Arbitrary orientation

The following step is to consider the ellipsoids not all parallel; since they are usually many, there is no point in defining the orientation of each one; instead is necessary to introduce a distribution function, that represent the relative density of ellipsoid with a certain orientation.

Again, the simplification from ellipsoid to spheroid is critical to achieve a reasonably compact description of the orientation; let's imagine the spheroid as a needle with an arrow on his tip, see figure 2.5:

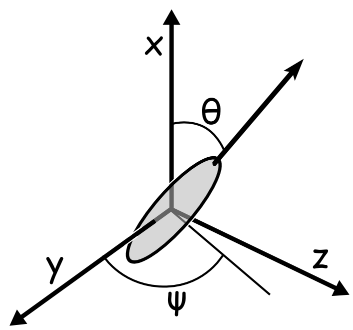

Figure 2.5: Definition of the orientation angles θ and ψ with respect to an arbitrarily oriented frame. A third angle is not needed since the spheroid is invariant around its main axis. Note that the angle θ is measured from x axis and not from yz plane; this choice is very convenient when the magnetic field is turned on along the x axis.[110]

The orientation is thus defined by a single direction vector, that spans a solid angle Ω. Due to the mirror symmetry of the spheroid (and of the material of which is made, which is assumed isotropic), the orientation can be reduced to half sphere, $0 \leq \psi \leq 2\pi$, $0 \leq \theta \leq \pi/2$. Let $P(\Omega)$ be the probability density of for a spheroid to be oriented with angle Ω; the normalization condition is:

$$1 = \int_{\Omega} \mathrm{d}\Omega P(\Omega) = \int_{\theta=0}^{\pi/2} \mathrm{d}\theta \int_{\psi=0}^{2\pi} \mathrm{d}\psi \cos\theta \; p(\theta, \psi) \tag{2.10}$$

Then, let's rewrite the effective equation (2.8) for a generic orientation of the spheroid, meaning rotating the linear tensor (2.9), like from the figure 2.5; the rotation is here performed only around the θ angle, otherwise is too complex, and the ψ will be shown to be essentially superfluous and is set to 0:

$$\begin{aligned}\chi_{eff}(\theta) &= \mathbf{R}\chi_{eff}\mathbf{R}^{-1} \\ &= \begin{pmatrix}\cos\theta & -\sin\theta & 0 \\ \sin\theta & \cos\theta & 0 \\ 0 & 0 & 1\end{pmatrix} \cdot \begin{pmatrix}\chi_a & 0 & 0 \\ 0 & \chi_b & 0 \\ 0 & 0 & \chi_c\end{pmatrix} \cdot \begin{pmatrix}\cos\theta & \sin\theta & 0 \\ -sin\theta & \cos\theta & 0 \\ 0 & 0 & 1\end{pmatrix} \\ &= \begin{pmatrix}\chi_a\cos^2\theta + \chi_b\sin^2\theta & (\chi_a - \chi_b)\cos\theta\sin\theta & 0 \\ (\chi_a - \chi_b)\cos\theta\sin\theta & \chi_a\sin^2\theta + \chi_b\cos^2\theta & 0 \\ 0 & 0 & \chi_c\end{pmatrix}\end{aligned} \tag{2.11}$$

Thanks to the general linearity of electromagnetism, is now possible to get the average (tensorial) permittivity by integrating this expression over the distribution of orientation; in the following formula the integration goes separately for all 9 components of the χ; and the $p(\theta, \psi))$ is considered constant in ψ:

$$\chi_{ave} = \int_{\theta=0}^{\pi/2} \mathrm{d}\theta \int_{\psi=0}^{2\pi} \mathrm{d}\psi \cos\theta P(\theta,\psi) \; = \; 2\pi \int_{\theta=0}^{\pi/2} \mathrm{d}\theta \sin\theta p(\theta)\chi_{eff}(\theta,\psi) \tag{2.12}$$

The fact that $P(\theta, \psi)$ is constant in ψ mean that the distribution is invariant for rotations around the z axis; with this consideration, can be stated that the off-diagonal components of χ_{ave} vanish. The interest is then all in the xx component, that can be written explicitly:

$$\chi_{ave}^{xx} = 2\pi \int_{\theta=0}^{\pi/2} \mathrm{d}\theta \sin\theta p(\theta)(\chi_a\cos^2\theta + \chi_b\sin^2\theta) \tag{2.13}$$

This result is used to evaluate the effective permittivity when a field is imposed in the z direction. In the special case when all ellipsoids are aligned with the z axis, θ is $\pi/2$ for them all, and the distribution has a Dirichelet δ shape $p(\theta) = \delta(\pi/2)/(2\pi)$ (some normalization..), and the special case of equation (2.8) is obtained again. Another special case of paramount interest is when the ellipsoids are oriented randomly,

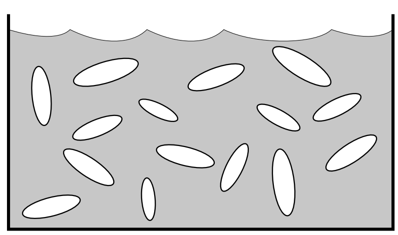

Figure 2.6: A suspension with randomly oriented particles ellipsoid, represented in 2D. On large scale it should look isotropic.[107]

see figure 2.6 that is the reasonable case when the suspension is throughly mixed. In this condition $P(\Omega)$ is constant, meaning also $p(\theta, \psi)$ to be constant and from the normalization, to be $1/(2\pi)$; the integral can then be solved[5]:

$$\chi_{ave}^{xx} = 2\pi \int_{\theta=0}^{\pi/2} d\theta \sin\theta \frac{1}{2\pi}(\chi_a \cos^2\theta + \chi_b \sin^2\theta) = \frac{1}{3}\chi_a + \frac{2}{3}\chi_b \tag{2.14}$$

Beautiful! To touch with hand the results, it is instructive to see how this formulation behave with limiting cases, meaning very long ellipsoids (called needles) or very flattened ones, like coins, for which the depolarizing factors has a simple value.

2.3.3 Needles and coins

Let's take the ellipsoid with the shape of a needle; from the table C.1 comes $N_a = 0$, $N_b = 1/2$, Thus the effective permeabilities along a and b axis are, given χ the one of the material, and δ the concentration

$$\begin{aligned} \chi_a &= \delta\,\chi \\ \chi_b &= \frac{\delta\chi}{1+\chi\frac{1-\delta}{2}} \end{aligned} \tag{2.15}$$

Thus, when all the needles are aligned along the field x, the average is the same :

$$\chi_{ave}^{xx} = \delta\,\chi \tag{2.16}$$

While when the needles are randomly oriented,

$$\chi_{ave}^{xx} = \frac{1}{3}\delta\,\chi + \frac{2}{3}\frac{\delta\chi}{1+\chi\frac{1-\delta}{2}} = \frac{1}{3}\delta\chi\frac{6+\chi(1-\delta)}{1+\chi\cdot\frac{1-\delta}{2}} \tag{2.17}$$

Let's do also the case of flat disks, coins or platelet, in which $N_a = 1,\ N_b = 0$; this is of special interest in case of one of the main ingredients of the drilling mud, the Bentonite [6]. The demagnetizing factors are:

$$\begin{aligned} \chi_a &= \frac{\delta\chi}{1+\chi(1-\delta)} \\ \chi_b &= \delta\,\chi \end{aligned} \tag{2.18}$$

so when they're all aligned flat, perpendicular to the field (so the short axis a is parallel to the field), the effective permittivity is:

$$\chi_{ave}^{xx} = \frac{\delta\chi}{1+\chi(1-\delta)} \tag{2.19}$$

[5] This integral could be avoided, by saying that the random distribution is isotropic, so must be the average: $\chi_{ave}^{xx} = \chi_{ave}^{yy} = chi_{ave}^{zz} = 1/3\chi_a + 1/3\chi_b + 1/3\chi_c$, with $\chi_c = \chi_b$ for the spheroid. The match of the two results encourages to use the integral for more complex tasks.

[6] Must be reminded that when mixed with water, the clay Bentonite swallows a lot of water and separates in platelets of *one molecule thick*, creating a strong gel. Its magnetic properties (as measured in the dry bulk) come from a variable contamination of Iron. Iron atoms are trapped and dispersed between the platelets, making the model of a compact macroscopic platelet, with uniform susceptibility, not so realistic.

While when they're randomly oriented

$$\chi_{ave}^{xx} = \frac{1}{3}\frac{\delta\chi}{1+\chi(1-\delta)} + \frac{2}{3}\delta\,\chi = \frac{1}{3}\delta\chi\frac{3+2\chi(1-\delta)}{1+\chi(1-\delta)} \tag{2.20}$$

for the platelets, is interesting also the case when they are oriented with one of the long axis parallel to the field:

$$\chi_{ave}^{xx} = \delta\chi \tag{2.21}$$

All those relations are very clean, and could be ready to be used directly in practical applications. It is however time to disclose the worst calculation of all this thesis. As already indicated, the susceptibility for all materials is very small, except some ones containing Iron (or Cobalt, or Rare Earths[7]). It is very instructive to calculate how those relations behave for χ small. Now, computing the approximate form of equations (2.16), or (2.17), and (2.19), (2.20),leads to the same result for them all:

$$\chi_{ave}^{xx} \simeq \delta\chi \tag{2.22}$$

That is again the simple, old weighted average formula (2.6)! This horrible consideration could relegate all the formulas, carefully evaluated for spheres, needles and platelets, in a remote corner: the hidden place for elaborate formulas with scarce use. The only good side is to know that such a simple average can be reliably used, without caring of the shape and orientation of the particles.

Furthermore, not all the effort was lost; the special case, when the suspended particles have a huge susceptibility, seems to really happen in the oil fields, as small quantities of iron compounds (metallic debris from the machinery, accidentally acquired Magnetite, etc.) sneak in the mixture, radically altering its magnetic response. In electrostatic the situation is different, since materials with high polarizability are the norm, and all the effort dedicated in the mixing formulas is mandatory, see figure 2.7.

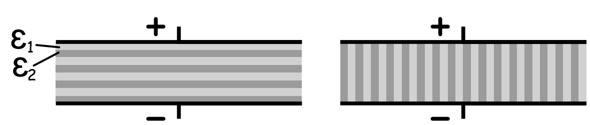

Figure 2.7: Two electric condenser, made with many plates of two different dielectrics. On the left, the horizontal configuration is equivalent to the model of platelets aligned flat, as in equation (2.19). In the right image, they are stacked vertical, reproducing the case of equation (2.21). With those simple configurations, the field can be computed exactly, and the effective dielectric constant should match the calculation made with the ellipsoids. In real condensers, there is few air, ϵ_1, and the main dielectric material, like a plastic, have a huge ϵ_2. The left configuration give rise to a stronger field, and is therefore chosen.[108]

[7] In the case that a relevant amount of Rare Earth's metals is found in the drilling mud, it is probably economically convenient stop the drilling and start selling those metals

3

Dynamic models

What if the particles in the suspension are free to move and can align with the magnetic field?

3.1 Dipoles alignment vs. Brownian motion

3.1.1 Application of Boltzmann distribution

As first model is the classical theory for a system of dipoles inside an uniform field. The dipoles are considered free to move, like in a rarefied gas, and are subject to the external field, that push to align them, and the random Brownian motion, that pulls in the opposite way, randomizing the direction of the dipoles. On average, who will win, in this battle between order and chaos?

The answer come from Statistical Physics, and is known as the theory of paramagnetism (or also of dielectric polarization) of gases; it is a neat application of the Boltzmann's energy distribution law, therefore illustrated in most books: [2, §28] [8, §3.1], [5, §6.3], [4, §52], and already applied to the drilling mud in the bachelor thesis by Leiros [22]. The classical model was developed originally by Langevin [42] and Debye [43] around 1900, and continuously developed since then.

The derivation of this model will be fast, following Böttcher [2]. Take a particle with a vectorial dipole momentum $\mathbf{m}$, when interacting with a field $\mathbf{H_e}$, has an energy:

$$U = -\mu_0 \mathbf{m} \cdot \mathbf{H}_e = -\mu_0 m H_e \cos\theta \tag{3.1}$$

Where m, H are the scalar values and θ the angle between the dipole and the field (in identical setup as in the figure 2.5). The field has the subscript e since it is not the external imposed field H_0, but the effective one that takes already into account the paramagnetism of the gas, meaning the influence of all dipoles that surround the one of study; at the end H_e will be evaluated; using directly H_0 here could lead to error when the induced magnetization is strong.

Boltzmann's energy distribution states that the probability density for a particle to be in a certain state is:

$$\mathrm{d}P = Ae^{-\frac{U}{K_b T}}\,\mathrm{d}\Omega \tag{3.2}$$

Where U is the energy of the state, in Joules [J] , T the temperature of the system in Kelvin [K] , k_b the Boltzmann's constant, $k_b \simeq 1.30 \times 10^{-23}\,[\mathrm{m^2ks^{-2}K^{-2}}]$. The $\mathrm{d}\Omega$ is the element of volume in the phase space and A is for normalization, such that the combination $A\,\mathrm{d}\Omega$ is non-dimensional.

The equation (3.3) can then be expressed in terms of the dipole energy [1]:

$$\mathrm{d}P = Ae^{\frac{U}{K_b T}}\,\mathrm{d}\Omega = Ae^{\frac{\mu_0 m H_e \cos\theta}{K_b T}}\sin\theta\;\mathrm{d}\psi\;\mathrm{d}\theta \tag{3.3}$$

This is a distribution of probability, and any value of interest can be obtained by integrating its value, multiplied for the probability weight, over all phase space. The degree of orientation of the particles (and thus the overall magnetization in the direction of $\mathbf{H}_0$) can be espressed as the average of $\cos\theta$ over the spherical solid angle of the possible dipole's orientations:

$$\overline{\cos\theta} = \int_\Omega \cos\theta\;\;\mathrm{d}P = \frac{\int_0^\pi \mathrm{d}\theta \int_0^{2\pi} \sin\theta\;\mathrm{d}\psi\;\;\cos\theta\, e^{\frac{\mu_0 m H_e \cos\theta}{K_b T}}}{\int_0^\pi \mathrm{d}\theta \int_0^{2\pi} \sin\theta\;\mathrm{d}\psi\;\,e^{\frac{\mu_0 m H_e \cos\theta}{K_b T}}} \tag{3.4}$$

Where the integral at the denominator is just the normalization factor A. Some variables can be grouped into a non-dimensional constant, that represent the ratio between magnetic and thermal energies:

$$\alpha = \frac{\mu_0 m H_e}{K_b T} \tag{3.5}$$

The integral (3.4) was solved long time ago, and gives as result:

$$\overline{\cos\theta} = \arctan a - \frac{1}{a} = L(a) \tag{3.6}$$

This is called the Langevin equation, for its first derivation in 1905. Let's see it looks in figure 3.1:

[1]For the application of Boltzmann theory to the magnetic energy of a macroscopic particle, one issue must be sorted out: let imagine this particle as a small magnetized bar, with the + at one tip and the − at the other. When the particle rotates, the dipole orientation rotates as well: it is coupled with the particle. And to rotate the dipole, the particle must be rotated. For the Boltzmann's law to be applied, the dipole orientation must be a separate degree of freedom, and a coupling with the physical rotation of the particles is likely to make the derivation very complex. Is therefore assumed here that the two rotations are decoupled. An argument in favour of this choice (other than the easier calculation) is that the particle of interest is big, thus its Brownian vibration are very small and fast compared to the almost macroscopic motion of orientation along the field. As proof, a needle of a compass will clearly orient to North, while at the same time performing tiny Brownian vibrations. This argument can be quantified, taking the rotational energy from the Equipartition Theorem $1/2\,k_B T$ [13] and thus the mean period of revolution of a (spherical) particle with density ρ is: $\overline{\tau} \approx 4\sqrt{\frac{\pi\rho r^5}{15\,k_B T}}$ For a particle 20 µm large, this period is about four seconds, while for 2 µm the period is down to one hundredth of second, that should still be well above the mean collision time.

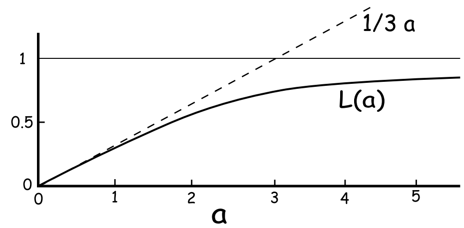

Figure 3.1: The well behaved plot of the Langevin formula as function of a. For a small is linear (paramagnetic region), while for a large the system reach saturation. With reference to this plot, a is **defined** small when it's ≤ 1, and large for $a \geq 5$. [104]

3.1.2 The magnetization from the dipoles

As defined before, the parameter a represent the ratio between magnetic and thermal energy. When a is big, the magnetic forces dominate, all particles align and the $\overline{\cos\theta} \approx 1$. On the opposite, when a is small (f. eks. the magnetic field is very weak), the particles do what they want, and their alignment disappears. Is very interesting to take the first order of $L(a)$ near zero, to obtain a linear relation, corresponding to the susceptibility of the ensemble. The result is the Curie law for magnetism, found ten years before Langevin's:

$$C(a) = \frac{1}{3}a = \frac{\mu_0 m H_e}{K_b T} \tag{3.7}$$

To translate those non-dimensional results into something real, must be introduced the average volumetric magnetization of the ensemble, obtained by summing the contribution of all dipoles, divided by the volume V:

$$\mathbf{M} = \frac{1}{V}\sum_i \mathbf{m}_i \tag{3.8}$$

Is then convenient to rewrite the particle's magnetic momentum in term of its volume $v = \frac{4}{3}\pi r^3$ (spherical particles), and average volumetric magnetization, called *remanence* $\mathbf{m} = v\mathbf{M}_f$, $m = vM_f$ and assume that all the particle have the same size and thus the same absolute moment m [2] (but can be in different directions!). Also, set δ the volumetric fraction of the particles compared to the total volume; then the average magnetization can be finally expressed:

$$\mathbf{M} = \delta M_f \int_\Omega \mathbf{m}\, \mathrm{d}P = \delta M_f \mathbf{H}_e\ L\Big(\frac{\frac{4}{3}\pi r^3 \mu_0 M_f H_e}{K_b T}\Big) \tag{3.9}$$

This last expression has all is needed, relating the average magnetization explicitly to all microscopical properties. It remain to be sorted out the resulting field, defined as $\mathbf{H}_e = \mathbf{H}_0 - \mathbf{M}$. This is a bit tricky for the whole formula, therefore is carried on only the case of rarefied gas, when $M \ll H_0$, leading to an error of the order of M/H_0.

$$\mathbf{H}_e \approx \mathbf{H}_0 - \delta M_f\ L\Big(\frac{\frac{4}{3}\pi r^3 \mu_0 M_f H_0}{K_b T}\Big) \tag{3.10}$$

[2] A more realistic distribution of different sizes of the particles may be computable also, but for sure more complex to handle.

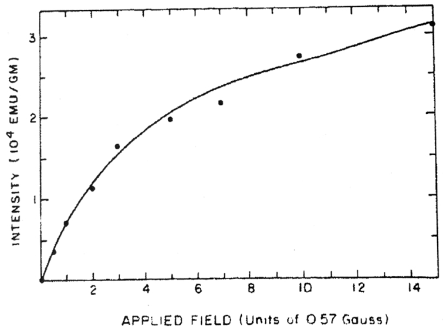

Figure 3.2: Experimental measures of the magnetization for a suspension of macroscopic dipoles. The Langevin function fits the data neatly, but is scaled with an ad-hoc factor. From Johnson and Murphy [62], year 1948. [112]

And this formula can be used to evaluate the effective field of a mixture that has been contaminated by a small amount of magnetized particles. The susceptibility cannot be defined, like from (2.1), since the relation is not linear (note the H_0 inside the Langevin function). It can anyway be linearized to the Curie's law (3.7), in the case of a weak field, high temperature and small particles:

$$\mathbf{H}_e \approx \mathbf{H}_0 \Big(1 - \frac{4\pi}{9} \frac{\mu_0 r^3 \delta M_f^2}{K_b T}\Big) \tag{3.11}$$

That is linear in the applied field, and can be used as well. The susceptibility can thus be defined, and will be χ_L, with L as Langevin:

$$\chi_L = \frac{4\pi}{9} \frac{\mu_0 r^3 \delta M_f^2}{K_b T} \tag{3.12}$$

A further interesting condition is that of the saturation, when all dipoles are tightly aligned. The magnetization is no more dependent on the imposed field:

$$\mathbf{H}_e \approx \mathbf{H}_0 - \delta M_f \tag{3.13}$$

3.1.3 Quantification

It must be evaluated which of the cases delineated in the previous section is likely to happen in the conditions found in the drilling mud. To do that, is necessary to quantify the parameters used; it is carried here a rough estimate, to understand the relative orders of magnitude. Accurate evaluations are postponed until the needed experimental data on the actual drilling mud components will be available.

As illustrated in the appendix B, the conditions of the drilling mud are: a fixed magnetic field, the Earth's one, of a strength $\mu_0 H_0$ of about 40 µT; a normal temperature of 300 K.

The magnetization, or better the remanence $R = \mu_0 M_f$ of those particles is highly variable, depending on detailed chemical composition, magnetization history and several other parameters. An upper bound is the remanence if the strongest permanent magnets manufactured, that is around 1.3 T, while a lower bound is more shaded. As representative value is chosen of 0.1 T, B. Dedicated measurements of the particle magnetization will be really welcome..

The particle size varies greatly, from molecular scale until grains of some millimeters; is then practical to evaluate the parameter a as function of the size. With the values indicated, the numerical relation for a results:

$$a(r, M_f, H_0, T) = \frac{\frac{4}{3}\pi r^3 \mu_0 M_f H_e}{K_b T} = r^3 \cdot 2 \times 10^{19} \tag{3.14}$$

Referring to figure 3.1, the linearized or Curie law (3.11) is a good approximation when the parameter $a \leq 1$, that happens when $r \leq 0.3$ [µm] , while the ensemble gets saturated for about $r \geq 0.6$ [µm] . Due to the power r^3, scaling down the remanence of the particle's material by a factor of 1000 (f.eks a weakly magnetized piece of steel) the r limits gets increased just by a factor of ten[3]. With a representative concentration of the contaminants of 1%, corresponding to the maximum concentration of Magnetite tested by Ding et al. [26], in the low-a range, the susceptibility (3.12) assume the value:

$$\chi_L(r, M_f, H_0, T) = \delta \frac{1}{3} \frac{M_f}{H_0} a = r^3 \cdot 1.1 \times 10^{18} \tag{3.15}$$

The big number at the end shouldn't scare, as the r is small: for $r = 0.3$ [µm] , $\chi_L \approx 10^{-3}$. In case the particles are large the saturation magnetization has the simple value:

$$R_s \approx \delta \; mu_0 M_f = 1000[\mu\text{T}] \tag{3.16}$$

That is huge, much bigger than the earth's field that is supposed to drive it. The error comes from the approximation of weak magnetization done in equation (3.10). Reviewing the calculations from that point should lead to a maximum magnetization equal to the imposed field, thus cancelling it, similarly to what happens for electric conductors in electrostatic. The medium will then behave as having *infinite susceptibility*, until the external field reach the ensemble's saturation limit[4].

The result is not compatible with the measures of [26]; at similar conclusion and mismatch arrives the paleomagnetism theory and experiments, [65, 7, 66, 74]. As consequence, the theory must be modified, and input data (specially the remanence of the particles) must be verified. Using a low value for the remanence of the material helps: if it is as low as 10^{-3} [T] , the saturation magnetization is 10 [µT] , that is nicer; but is not allowed to freely tune this parameter of the model, as it should be an experimental input.

On the other way, magnetic devices found in living organisms, as in figure 3.3, seem to confirm the theory,

[3] This scaling applies to the extension of the linear range, not to the amount of magnetization

[4] This situation of cancellation of the magnetic field is found also, for example, with on-purpose magnetic shielding systems, like the "Magnetic Faraday cages" to handle sensitive equipment. A deeper study on this subject will be very interesting, but for the sake of focus and compactness has to be skipped, this time.

at least locally; and experiments from paleomagnetism suggests that the dependency is good, but a strong scaling is needed, as shown in figure 3.2. The issue will be left open, hoping that it could constitute fertile ground for another future thesis. Some ideas that could lead to a solution are listed in the section 3.3.

Also the result of the linearized equation (3.11), with its susceptibility (3.15), is prone to the same error, and after having assessed the the obtained magnetization M must be checked to be much smaller than the driving field, and all the corrections included to the total alignment .

As was shown, the dipoles in suspension can have powerful magnetic effects; the use of the linear model 3.11 must be carefully limited to opportune conditions, and critical parameters like the size of the particles and the remanence of the material must be carefully assessed, as can dramatically change the behaviour of the system. Having checked those precautionary conditions, the formulas obtained are simple and explicit, and can be used.

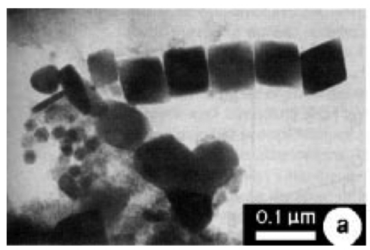

Figure 3.3: TEM image of a magnetosome, a row of magnetite crystals that some bacteria use as magnetic compass to orient themselves with the Earth's field. Pigeons, salmons and probably also humans have similar devices installed. Note the size, the smallest at which the magnetic orientation can be discerned from Brownian white noise, as from equation (3.14), with magnetization of small magnetite crystals as high as 1 [T] . Image from the Butler's book on Paleomagnetism, [7], who get it from C. McCabe. [99]

A last check for this model: assume the dipoles are (classical) iron atoms, with a (classical)[5] magnetic dipole of a magnitude of the Bohr's magneton, $\mu_b \simeq 9.3 \times 10^{-24}$ [J T^{-1}] . Dissolving iron atoms in water at a concentration by weight of 2.7 %, like in the experiment of Ding et al. [26], give rise to a numeric density of $n \approx 3.6 \times 10^{24}$ atoms per unit volume. The small Bohr magneton fit in the category of $a \ll 1$, then the susceptibility results:

$$\chi_I = n\,\mu_b \frac{\mu_b H_0}{k_b T} \simeq 2.3 \times 10^{-6} \tag{3.17}$$

That is small, but in the order of magnitude of the susceptibility of normal paramagnetic materials; this small value will reduce the Earth's field by an amount

$$\Delta H_0 = \chi_i\, H_0 \simeq 9 \times 10^{-5} [\mu\text{T}]$$

[5] As usual, no quantistic spin or orbit; furthermore, the magnetic moment of single atoms is crucially dependent by the chemical surrounding; and also, an atom is small, meaning its inertial rotational motion cannot be decoupled to the dipole alignment, unless is a real isolated atom; and so on. A derivation with quantistic magnetic moment will lead to the Brillouin function, qualitatively similar to the Langevin one. See [5, §7.8].

That is, so small to be undetectable and negligible; this estimate is confirmed by the experimental measurement in [26].

3.2 Alignment of paramagnetic ellipsoids vs. Brownian motion

The model presented in the previous section, the Langevin model for the orientation of a gas of fixed dipoles, can be adapted to be used for a suspension of paramagnetic particles. When a paramagnetic particle is subject to an external uniform magnetic field it will be subject to a torque that tends to align the it along the field, unless this particle is perfectly spherical. Approximating a non-spherical particles with an ellipsoid allows to calculate this torque; in the appendix C are sorted out all the details for the ellipsoid into an uniform field.

Similarly to the case of dipoles, the alignment of paramagnetic particles could greatly influence the mean magnetization of the system. The development of an orientation model for paramagnetic particles was the main goal of this thesis work, since it was identified as a key process that can influence the magnetization of the drilling mud [25], with the particles represented by iron compounds, with very high susceptibility. A first approach to build a thermodynamic model has been presented in the bachelor thesis by Leiros [22], like for the Langevin model, and here is expanded.

Most of the physical basis are already set up, in the previous sections and in the appendix C. Instead of the dipole energy (3.1), the energy for the interaction between the ellipsoid and the external field must be used, as from equation (C.15):

$$U_r = k\,\cos^2\theta \tag{3.18}$$

Note the $\cos^2\theta$ here instead of just $\cos\theta$ from the dipole (3.1). In the factor k are condensed all the features of the ellipsoid, (C.16).

The energy so defined can be put into the Boltzmann distribution formula, as was done for the dipole[6]. There are a number of delicate issues about the Brownian motion of an ellipsoid, for which there is no space here; the error caused by ignoring all those consideration should be manageable; see for example [44, 55, 59] the probability density, as function of the angle θ between the field $\mathbf{H}_0$ and the ellipsoid axis a (refer always to the figure 2.5 reads[7]:

$$\mathrm{d}P = A\,e^{-\frac{k\,\cos^2\theta}{K_b T}}\,\sin\theta\;\mathrm{d}\psi\;\mathrm{d}\theta \tag{3.19}$$

Now, what is looked for is the effective permittivity of the system (the "gas of ellipsoids"), given the distri-

[6] The model for paramagnetic particles was set up before realizing that Langevin did already the same for fixed dipoles; it is now positioned after because, well, Langevin did its model in 1905, and the paramagnetic ellipsoid is more tricky than a fixed dipole.

[7] In the equations following, k is the ellipsoid coefficient and K_b indicate the Boltzmann constant; sorry for the confusing notation.

bution; comes in aid the mixing formula (2.13) from the previous chapter, reproduced here, where only the component along the field is of interest, as the other should be zero for symmetry arguments[8]:

$$\chi_{par} = 2\pi \int_{\theta=0}^{\pi/2} \mathrm{d}\theta \, \sin\theta \, , p(\theta) \, (\chi_a \cos^2\theta + \chi_b \sin^2\theta) \tag{3.20}$$

The probability density (3.19) can be dropped into the integral (3.20), and taking care also of the normalization constant A, the whole construction will look like (3.4):

$$\chi_{par} = \frac{\int_0^{\pi} \mathrm{d}\theta \int_0^{2\pi} \sin\theta \, \mathrm{d}\psi \, (\chi_a \cos^2\theta + \chi_b \sin^2\theta) \cdot e^{-\frac{k \cos^2\theta}{K_b T}}}{\int_0^{\pi} \mathrm{d}\theta \int_0^{2\pi} \sin\theta \, \mathrm{d}\psi \, e^{-\frac{k \cos^2\theta}{K_b T}}} \tag{3.21}$$

This horrible expression is not so bad as it looks, specially if the variables at the exponential can be grouped, like was done for the Langevin derivation (3.5), into a non-dimensional constant that represent the ratio between the paramagnetic inclination energy and the thermal one:

$$c = \frac{k}{K_b T} \tag{3.22}$$

And a substitution of the variable of integration, $x = \cos\theta \;\; \mathrm{d}x = -\sin\theta \, \mathrm{d}\theta$, will do the rest, leaving two Gaussian integrals, that are widely accepted as normal functions and can be sorted out, giving as result[9]:

$$\chi_{par} = \frac{(\chi_a - \chi_b)\, e^c}{\sqrt{\pi c}\, \mathrm{erfi}(\sqrt{c})} - \frac{\chi_a - \chi_b}{2\, c} + \chi_b \tag{3.23}$$

This equation express the effective susceptibility of a suspension of ellipsoids, while is taken into account their desire to move[10]. The erfi is the imaginary error function. This expression still looks a bit scary, but is really well behaved in reality. It is convenient to rewrite it in term of a function $A(c)$ that groups all the weird dependencies:

$$\chi_{par} = (\chi_a - \chi_b)\, A(c) + \chi_b \tag{3.24}$$

As short consistency check, let reduce the ellipsoids to spheres, for which $\chi_a - \chi_b = 0$; the susceptibility takes the simple form:

$$\chi_{par} = \chi_b = \frac{3\,\delta\,\chi}{3 + \chi(1-\delta)}$$

That was the simple mixing formula (2.5), not dependent on the external field, confirming that there is no way to orient an isotropic sphere. .

[8]In effect, the formula (2.13) was introduced and specifically trimmed mostly to be used here, with the Boltzmann distribution.

[9]This result was originally obtained by using the powerful method of the *partition function* [22], [5, §7]; the direct derivation presented here is a little harder, but linear and doesn't involve much introduction of statistical physics concepts.

[10]The term *susceptibility* is slightly abused, as χ_{par} depends on the applied field H_0 through the c constant

3.2.1 Quantification

The function $A(c)$ have a very nice plot, illustrated in the figure 3.4: Referring to this figure[11], a set of

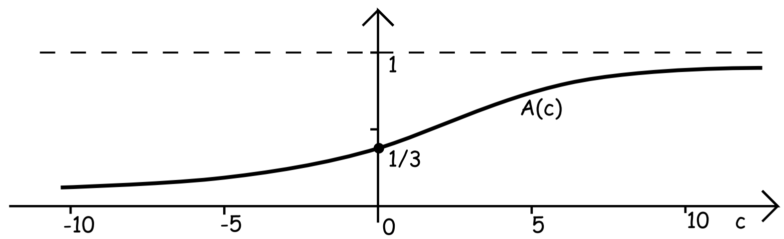

Figure 3.4: The function $A(c)$. No divergences nor renormalization issues, just a long and smooth s. [103]

considerations can be drawn. At first, let remind that $c > 0$ is the case of a paramagnetic particle, $\chi < 0$ that is attracted by the field, while $c < 0$ is the diamagnetic case, $\chi < 0$, that is of scarce interest.

When $c = 0$ the function has value $A(0) = 1/3$, meaning there is no magnetic field, reconducting to the susceptibility of randomly oriented ellipsoids, equation (2.14):

$$\chi_{par} = (\chi_a - \chi_b) \cdot \frac{1}{3} + \chi_b = \frac{1}{3}\chi_a + \frac{2}{3}\chi_b \tag{3.25}$$

Furthermore, for c small, the susceptibility can be said to be approximately constant with value from (3.25), that is quite simple; for more accuracy, a first derivative could be added, but it is not mandatory.
For c large, meaning when the magnetic field is strong, $A(c) \rightarrow 1$, and the condition where all the particles are oriented is reached, as equation (2.8):

$$\chi_{par} = (\chi_a - \chi_b) \cdot 1 + \chi_b = \chi_a \tag{3.26}$$

The alignment behaviour of the paramagnetic ellipsoids is then simple, predictable and not weird. Is interesting to understand when the conditions of c small or big happens. Let's set, with reference to the plot of $A(c)$ that $0 \leq c \leq 1$ is the 'small' range and when $c \geq 5$ is considered large.
Is then needed to get c explicitly: from the definition of c in (3.22) and in (C.16) for the k factor:

$$c = \frac{k}{K_b T} = \frac{\frac{1}{2} V \mu_0 \chi(\chi+1) H_0^2 \frac{N_a - N_b}{\left(1+N_a\chi\right)\left(1+N_b\chi\right)}}{K_b T} \tag{3.27}$$

And taking the limit case of a long and thin ellipsoid, the needle, with the N_i coefficients from table C.1:

$$c = \mu_0 \frac{2\pi}{3} \frac{r^3 H_0^2}{K_b T} \frac{\chi(\chi+1)}{\chi+2} \tag{3.28}$$

[11]The analysis of the function is omitted, as quite long and tricky. The unsurprising results are condensed in the plot.

Extracting the radius of the particle r[12]:

$$r = \Big(\frac{3}{2\pi} \frac{c\, K_b T}{\mu_0\, H_0^2} \frac{\chi + 2}{\chi(\chi+1)} \Big)^{1/3} \tag{3.29}$$

With the a value for the susceptibility of the particle $\chi = 10$, like steel filings in appendix B the value of r results:

$$2r < 10[\text{mm}] \;\Rightarrow\; c < 1 \qquad 2r > 20[\text{mm}] \;\Rightarrow\; c > 1 \tag{3.30}$$

Thus, paramagnetic particles up to the size of ten [mm] will not orient significantly, and with double size are almost perfectly aligned. This size is much more than what was expected; particles of ten [mm] are likely to be eliminated by the mud system, and chunks of steel of such size will not remain unobserved, or aren't likely to stay suspended in the fluid.

Taking a larger χ will help a bit to reduce the size of the particles to see the effect, bu not too much since $r \sim \chi^{-1/3}$. With the great value of $\chi = 10^5$, the minimum size to see the orienting is 0.4 [mm] , now almost in the range of a suspended solid. Similarly to the case of suspended dipoles, the knowledge of the magnetic properties of the contaminants is mandatory to apply the model.

A difference between the two models must be observed: in the dipole model the state of random orientations correspond to zero magnetization; for the suspension of paramagnets, the things are going differently: at random orientation the susceptibility is already considerable, and is only increased of something with the alignment. For the case of needles, the maximum susceptibility (3.26) is about three times the minimum one (3.25), in the limit case of large χ. This observation will turn useful to interpret the experimental result of the next section.

3.3 The dynamic shielding

"With four parameters I can fit an elephant, and with five I can make him wiggle his trunk."

– Probably John von Neumann

In this last section is addressed a puzzling experimental result, that hardly fits into rational models. Here method of careful derivation from first principle is abandoned, in favour of creative and qualitative fitting of the experimental evidence. No accurate or predictive calculations are sought: the territory is vastly unexplored, and just a rough map will be sketched.

After two chapters of detailed coefficients, integrals and ellipsoids, it is time now to have some fun and just play with physics instead of working on it.

[12]For the following calculation, the radius is calculated from the volume considering the particle as spherical. But it was a needle the equation before! After the Spherical Cow, here it is the spherical needle. Anyway, is just to estimate the size. A needle of same volume will be a bit longer, say an order of magnitude, but no more.

All the models developed up to now were static; the particles are allowed to move, but the fluid, in the large scale, is still, and the magnetic field is fixed. In real drilling practice the situation is quite different: the mud is pumped and mixed at high speed, and just before taking the magnetic measures, the circulation is usually stopped, and the mud become still. That condition was reproduced in the experiment reported by [26, 25]. A bucket of mud was mixed, a magnetometer inserted, and the mud left at rest. The readings of the magnetometers, as function of time, are illustrated in the figure 3.5. As shown from the figure 3.5, the

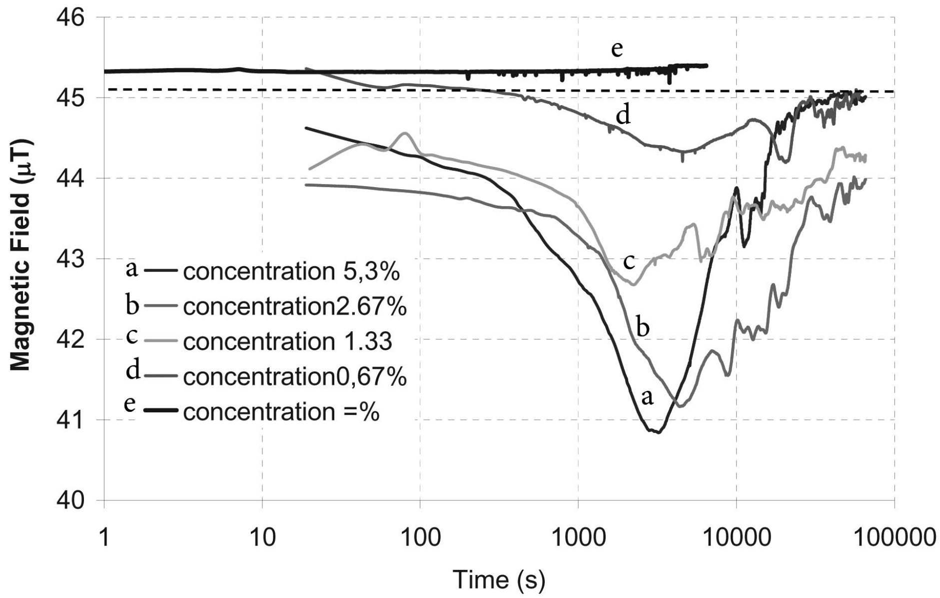

Figure 3.5: The experimental evidence: time variation of the magnetic field inside a bucket of drilling mud, after it was mixed at $t = 0$, from [26]. Different lines are different experiments, varying the concentration of the contaminant, magnetite. [101]

measured field varies with time, consistently in several experiments, and the time dependency is not trivial. How to explain this behaviour? The answer is qualitative and graphic, depicted in the figure 3.6: The idea

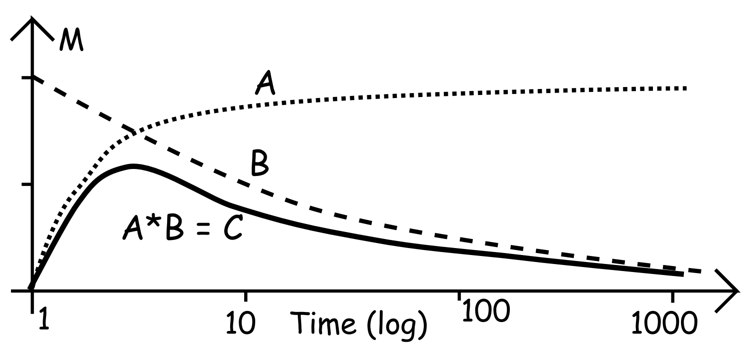

Figure 3.6: Two uni-directional processes A and B, combined, can model the magnetization $C = A * B$. The measured field in 3.5 is obtained by flipping C. [102]

of figure 3.6 is to split the process into two: the process A, represented by a progressive and increasing magnetization of the mud; the process B, that operate a progressive and slower damping on the process A.

3.3.1 The retarded magnetization

The best candidate to represent a progressive magnetization is the alignment of the suspended particles. The mixing is assumed to destroy the orientation of the particles. When the mixing is stopped, the alignment starts, but is not immediate: the viscosity if the fluid slows the motion, together with the Brownian disturbance.

The viscous term can be sorted out in good detail, with some assumptions: the fluid is to be Newtonian, the mass forces are set negligible to the viscous ones, and the particle is, again, ellipsoidal. The motion of an ellipsoid in a fluid can be solved exactly [11], with the same methods of appendix C!

The result for a pure rotation motion in a fluid should look like that: a torque, linear with the rotational speed of the particle, and directed against it; plus a weird numerical coefficient in front, to remind that the ellipsoid is not trivial.

The magnetic torque can be obtained by differentiating the energy used for the dipole (3.1), or from the paramagnetic ellipsoid model(3.18). The first give a $\sin\theta$, ad the second a funny $\sin 2\theta$. The magnetic force acts against the viscous one, thus generating a first order equation:

$$\dot{\theta} = q \sin(\theta) \tag{3.31}$$

This first is for the dipole; in the parameter q there are all the coefficients of the case, that are not computed here. For the paramagnetic ellipsoid, the dynamics is governed by:

$$\dot{\theta} = p \sin(2\theta) \tag{3.32}$$

Those equations could be solved[13] and a nice solution is expected, with the particles aligning with the field and θ approaching zero as time passes.

The resultant magnetization dynamics can then be evaluated, by setting as start condition a random distribution; the instantaneous average magnetization is obtained by the equation (2.13) for the paramagnet and a version of (3.4) for the dipole. Will the functions look qualitatively like the A in figure 3.6?

There is a difference between the paramagnetic and the dipole case, as already mentioned: A random distribution of dipoles has zero magnetization; while the random distribution of paramagnetic ellipsoids has a finite and significant susceptibility. That susceptibility give immediate rise to magnetization; thus, a suspension of paramagnetic particles will show immediate damping of the field, and a time strengthening of the damping limited to maximum three times of the initial one, that is approximately incompatible with the experimental results.

[13] The supervisor say that they are almost trivial.

The dipole model can start from zero, and passes the test.

A proper treatment of the Brownian dynamics of the alignment is expected to be more complex than the viscous force [15]; let's assume that the essential contribution of all the Brownian details is just to make a bit more complex the coefficient obtained from the viscous model. With that last simple step, the model for the retarded magnetization A could be said complete.

It was easy! Well, no details were sorted out, and no quantitative prediction is available; all still rely just on arguments, and will need a lot of work to become really useful. But that's all, for now.

3.3.2 The damping

The modelling of the process A, the retarded magnetization, was just a draft. The modelling of the process B, a slow but definitive damping of the magnetization, will be just a list of ideas. Note that a model for the damping of suspended dipoles is also needed for solving the problem left open with equation (3.16).

A process is needed that slowly damps the magnetization carried by the dipoles, up to almost cancelling it. No one of the models already discussed in the previous sections can provide such a damping. Something different is needed, and there are several ideas on how to do that:

Remove

If the particles are removed from the mud, they won't affect the magnetization anymore. The first process is sagging, or falling of the particles at the bottom of the bucket, leaving the mud free. It is very attractive, since the simple Stoke's law [11] is available to get the falling speed of particles and thus the. But the experimenters don't agree: there was no sagging. The mud is thick and holds all the particles during the experiment.

Another way to eliminate solids is to dissolve them; iron and magnetite are unstable in water, and after a while they will disappear. But again, the reality say no: the experiment was repeated remixing the same mud, and all worked as before, so the particles are still there. How else could they disappear? Are made of Iron, so nuclear decay is out of discussion.

Block

Another idea comes from the thickness itself of the mud. When flows, the mud has low viscosity, but when is left still, the thickeners and gelling agents slowly build a solid network, creating a brown pudding. The magnetic particles can remains trapped in the network, n more able to follow their magnetic desire, or even forced to take unnatural positions by the tightening gel. This theory is promising and not confuted jet; the magnitude of the forces could be derived from the macroscopic gel strength, and some data taken from the paleomagnetism [74].

Shield

A grain of magnetite, seen from near, possess a very strong magnetic field; such field can alter the linear response of the neighbourhood, that shields the magnetic field of the particle; this secondary shielding must be slower than the grain orientation; is quite strange since almost all non-linearities involve a decreasing of the susceptibilities increasing the field, while here is needed the opposite.

A possibility could come from the vast and fertile land of surface chemistry: the layer that wraps the magnetic particles could slowly became superparamagnetic (or superconductive, should be good as well) for some obscure reason, in a slow and delicate manner, thus shielding each particle field.

Chain

As happen in ferrofluids, the small magnets that roam in the fluid can meet and attach each other; since the local magnetic forces are much stronger than the feeble Earth's field, they will not follow a plan, and will assemble in disordered clusters of rings that annihilate each other's field; the bond is not so strong and can be disrupted by mixing.

And could be added more mechanisms; many of the ideas may seem unrealistic, but must be reminded that an official model hasn't been settled yet; the physics of small things is so rich and surprising, that no roads should be left unexplored for the fear of a mistake. At worst, something unexpected could be discovered.

□

4

Summary and Recommendations for Further Work

4.1 Summary

The main topics addressed in the thesis are shortly repeated here, in comparison with the Objectives that were set in the section 1.2. The previous models for the drilling mud have been reviewed, in particular: the *Wiedemann law* approach, for the susceptibility of a mixture, is expanded to a general mixing model, and are assessed the ranges of applicability.

The models of orientation of the suspended particles were developed in detail, compared to the relevant literature, and their main predictions confronted with the available data.

An extensive research in the literature was carried, identifying a great number of fields of science that deals with magnetized ellipsoid and effective susceptibility; and including also the electrostatic twin problem, the amount of interesting work done is amazing. A detailed literature survey is not reported for reasons of space; main useful contributions gained are the Mixing formulas of chap. 2, a good assessment of Langevin theory in the first part of chap. 3, data from the experiments in paleomagnetism.

The core physics of the drilling mud linked to the illustrated models has been thoroughly exposed, deriving the relations from general priciples. However, the results obtained indicate that there are some complex key processes that are still unidentified. The experimental observation in the section 3.3 had only a drafted an partial explanation, and the current models are insufficient to interpret the process.

Several practical formulas are presented, and their applicability is discussed. The calculations are started from their natural origin, and carried with as many detailed steps as the space allows; but several derivations have been skipped, when repeated, too trivial or too complex. Specific reference is given to didactic manuals

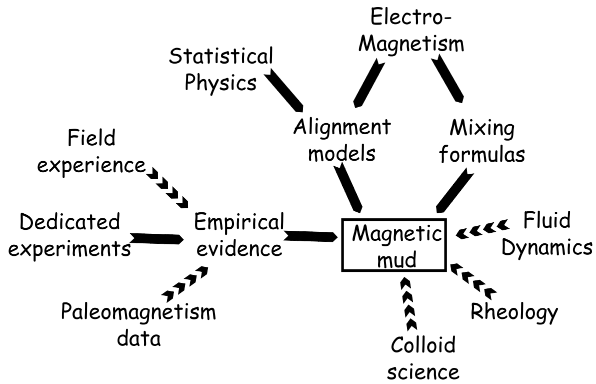

Figure 4.1: A scheme of the elements needed to model the magnetic properties of the drilling mud. Broken lines inserted where the connection is identified but not fully exploited. [106]

where needed.

The figure 4.1 is a synthetic representation of the work done.

4.2 Results for the impatients

For those who don't want to read the whole thesis, the essential results are listed here:

- When two substances are mixed, if their susceptibilities χ_1, χ_2 are close, is possible to use the Wiedemannn's law, the volume weighted average (2.22):

$$\overline{\chi} = \frac{\chi_1 V_1 + \chi_2 V_2}{V_1 + V_2}$$

- When a small volume fraction δ of a magnetic contaminant with high susceptibility χ is added to the mud, is better to use the Maxwell-Garnett formula, (2.5):

$$\overline{\chi} = \frac{3\,\delta\,\chi}{3 + \chi(1-\delta)}$$

- If a small fraction δ of fixed dipoles of remanence R is added, the magnetization is governed by the Langevin function (3.6):

$$M = \delta\,R\,L(a)$$

- If the contamination strongly magnetized material, like an industrial magnet grinded, is added, the mud should be capable of shielding completely the Earth's field (**??**).
- But unidentified processes normally hamper that effect.
- If a small fraction of large paramagnetic particles are added, the susceptibility could be expressed as

(3.24)

$$\chi_{par} = (\chi_a - \chi_b)\, A(c) + \chi_b$$

4.3 Recommendations for Further Work

The magnetic properties of the drilling mud are still far from clear. Useful progresses will come by:

- Experimental assessing of the properties of the contaminants;
- Theoretical research on the chemical-physical interactions of the contaminants, with their interaction with the rest of the mud;
- Extension of the basic models for distributions of sizes and shapes.
- Integration of the paramagnetic and fixed-dipole models into a single, flexible model for ferromagnetic materials.

≈

Appendix A

The Drilling Mud

In this appendix are shortly described the Drilling Mud and the magnetic contaminants that it could acquire.

A science on its own

The drilling mud is the liquid that is pumped in the well during drilling; its importance in the technology of drilling and in the expense budget is so relevant that has create a whole field of science of its own, see for example the book [14]. This specially tailored and expensive fluid performs several duties, the most important of which are:

- Lubricate the drilling bit;
- Transport to the surface the *cuttings*;
- Compensate the *geological pressure* in the well;

And many other duties, like avoiding corrosion, allow easy separation of the cuttings at the surface, etc.

The liquid that constitute the bulk of the mud is called the *base*, and could be either water, oil, or synthetic fluids, and even a mixture of those.

To properly transport upward the cuttings, the mud must possess a jelly consistence, and the proper rheology [6] is obtained with additives like the clay *Bentonite* and polymeric gelling agents. The complex composition and the markedly non-newtonian consistence of this fluid could play a significant role in the movement of the magnetic particles described in the chapter 3.

To compensate the geological pressure, often the fluid is needed to be heavier than the water, and *weighting additives* are used, like the mineral *Barite*. And then, another thousand of chemicals or empirically-based additives to achieve all the most intricate properties needed.

The mud is usually processed at the rig with a dedicated system and then reused. The main components of the *mud system* are:

- The *shale shaker*, that filters the coarse solids coming out of the well;
- The *mud pit*, where the fluid is stored and decantate;
- The *mud pump*, that sucks the fluid from the pit and send it down in the well.

Often there are many other components in the mud system; one of them, of great interest for the magnetic problems, is the *ditch magnet*: a grid of powerful magnet set against the stream of mud, in order to attract and remove from the mud the coarsest magnetic particles.

Magnetic contaminants

A freshly prepared mud is usually non-magnetic, with a very small susceptibility. As first exception to this rule, if as weighting agents are used the uncommon *Ilmenite* from Sokndal [17], or the *Hematite* mineral, that have both strong magnetic properties, the resulting mud will be magnetic.

The second exception is the widespread addition of Bentonite, that has weak paramagnetic properties due to a variable Iron content. Bentonite can give a significant contribution to the mud's susceptibility [30].

Leaving apart those manageable exceptions, in normal conditions the magnetic contribution comes from uncontrolled contamination, thanks to a great variety of potential sources:

- Steel swarfs comes regularly from the wear of the equipment, like the pumps, the drill string, the movimentation equipment;
- The rock formation being drilled can contain natural Magnetite or Hematite, that is acquired by the mud;
- The ingredients are often transported or stocked improperly, acquiring iron residues;
- Many ingredients employed have a proprietary formulation, and could contain iron.

The ditch magnet mentioned earlier are usually engineered to remove only the largest particles, and will leave all the fine ones in the mud. The special thickness of the mud allows relatively large particles to stay in suspension, and understanding the physics of this suspension of minute magnetic particles is the purpose of this thesis. The general term 'magnetic particles' is used, and its examples most often found in the mud are the small steel swarfs, Magnetite or Hematite crystals and Bentonite flakes.

Appendix B

Experimental values

In this appendix are summarized the representative numerical values found in the literature, that are used to quantify the models developed for the drilling mud. The amounts are to be considered only indicative, as the key magnetic properties of susceptibility and remanence have a wide range of variation for ferrous materials, that possess highly non-linear response, and not many specific experimental data are available. A simple numerical value is chosen within the range, to be used in the calculations.

For the Earth's magnetic field, the average value of 40 [T] is used [95], and the temperature is set to a normal ambient one of of 300 K[1].

The concentration of the magnetic contaminants is set to 1% by volume, about the maximum that was tested [26, 28], while in real situation the concentration is commonly much lower [18].

The size of the suspended magnetic particles is not defined, and could range from molecular scale to some millimeters. In the evaluations, the size is usually left as the main independent variable.

Paramagnetic materials

Material	Susceptibility range SI	Chosen value SI	Source
Water	9×10^{-6}	0	[82]
Steel	10^{2} - 10^{5}	10^{2}	[26],[82]
Magnetite	10^{-1} - 10^{3}	1	[26]
Bentonite	10^{-6} - 10^{-4}	10^{-4}	[84]

[1] Drilling mud could be very hot down in the well, but for simplicity the temperature is set to a normal ambient one of 23°C, as could be experienced in Norway during some warm summers.

Permanent magnets

Material	Remanence range [T]	Chosen value [T]	Source
Artificial magnet	10^{-1} - 1.35	10^{-1}	[94]
Steel	0 - 1	10^{-3}	[94]
Magnetite, chunks	0 - 1	10^{-1}	ND
Single-domain Magnetite	0.5 - 1	1	[7]

Appendix C

The Paramagnetic Ellipsoid

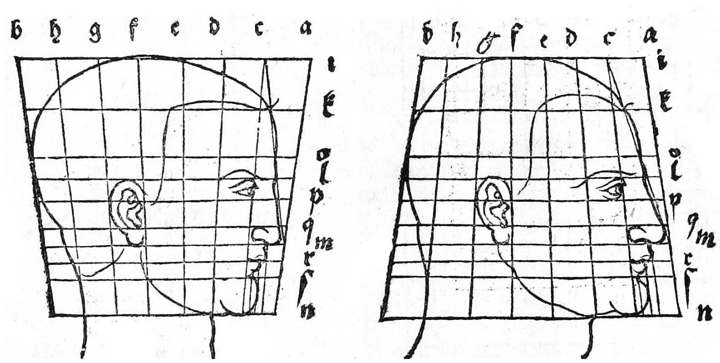

Figure C.1: *Face Transformations*, by Albrecht Dürer 1528. Geometric deformations are a powerful tool, widely used in art, topology, natural evolution and electromagnetism.[96]

In this appendix is reported the solution of the classical problem of a paramagnetic ellipsoid immersed on a medium of different susceptibility, when is applied an external static and uniform magnetic field. The rotational momentum that align the ellipsoid along the field is then derived.

The ellipsoid in uniform field is of historical and practical importance since it is one of the few analytically soluble problems of magnetostatic, due to its similarity with a sphere, see Figure C.1. Its results can be extended, with good approximation, to a wide array of shapes. It is useful to reproduce the solution here in order to show the key features and define clearly the notation.

Our magnetostatic problem is mathematically identical to the electrostatic one, and consists on solving the Laplace equation for an ellipsoid. The analytical challenge was first solved probably by Mathieu [39] in 1868, who was interested on the vibrations of an elliptical drum. He introduced the elliptical coordinates, that allow a natural implementation of the boundary conditions of our ellipsoid. The best "modern" presentation is found in the classical book by Stratton [1], who starts by solving a conducting ellipsoid in electrostatic field, then apply the proper corrections for a dielectric and finally for our paramagnet in static magnetic field. I will follow Stratton, except from some conventions that are cleaner in the Landau 8 [3]. A complete solution of this classical problem is usually lacking in the recent electromagnetism textbooks, probably because the Laplace equation has been effectively implemented in finite-element solver or because the passion for analytical details has been falling since some decades.

Anyway, detailed calculations for our application have been also carried on already during past Thesis works here at UiS [23, 27] and the results can be found repeated also in journal publications [48, 51, 60]. So, what is the result? If we apply an uniform external field, inside the ellipsoid the field will be also uniform, but not in the same direction of the applied one! The change in direction is dependent on the relative susceptibilities and on the shape and orientation of the ellipsoid, making energetically convenient to stay aligned with the field. Furthermore, this solution allows an easy integration of the magnetization momentum, thanks to the fact that it is uniform inside the ellipsoid.

This clean solution has been widely used; its most notable application is to *measure* with great accuracy the susceptibility of materials, that have to be shaped into an ellipsoid and placed inside a reasonably uniform magnetic field.

An outline of the calculation is as follows:

- [1] Say that the static magnetic field can be described in term of a scalar potential that obey Laplace equation;
- [2] Write the Laplace equation in a way that allows the application of ellipsoidal boundary conditions;
- [3] Find generic solutions;
- [4] Adapt the solution for a paramagnet with external field;
- [5] Evaluate the quantities of interest, namely energy and torque.

C.1 Rewrite Laplace equation

"Mathematical Analysis is the true rational basis of the whole system of our positive knowledge."

– Auguste Comte, 1853

The solution for paramagnetic ellipsoid is given by Stratton [1] in the §4.19, but most of the calculations are anticipated by the electrostatic case. The magnetostatic problem can be represented by the scalar potential $\phi*$, [1, §4.16] that plays the same role as the electrostatic potential: it must be a solution of Laplace's equation, and on how to fond this solution is dedicated what follows.

First, let's define what the ellipsoid is: it is a sphere that has been deformed. It doesn't mean that any pebble or potato can be consider as an ellipsoid, since the deformation type is strictly defined; but in this thesis is essential that any pebble, potato or sand grain can be well approximated by an ellipsoid.

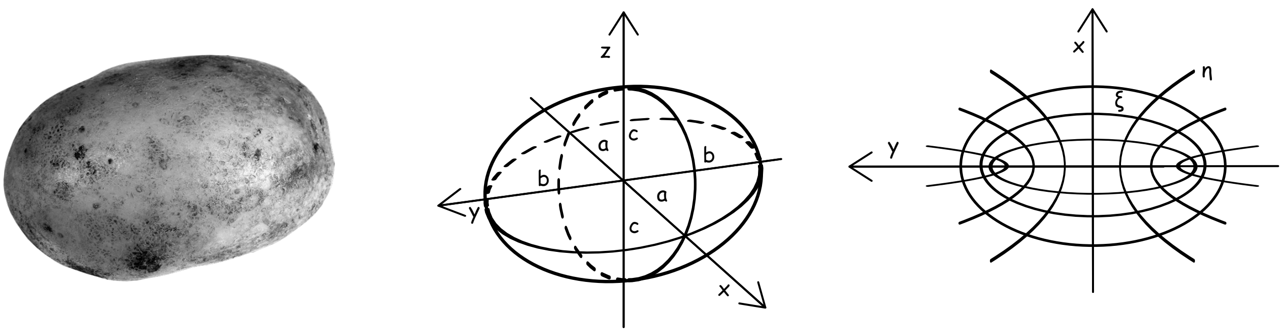

Figure C.2: A potato, an ellipsoid and a sketch of the elliptical coordinates in 2D. 3D ellipsoidal coordinates are obtained adding a further hyperboloid. Note the striking similarity between the ellipsoid and a generic potato. [109]

In cartesian coodinates (x, y, z) the ellipsoid surface is defined by the equation

$$\frac{x^2}{a^2} + \frac{y^2}{b^2} + \frac{z^2}{c^2} = 1$$

Where (a, b, c) are the semiaxes of the ellipsoid. Now, see [1, §1.18.8] or [3, §4], we can define the famous ellipsoidal coordinates introduced by Mathieu (and even sometimes called Mathieu coordinates). The ellipsoid equation can be slightly modified

$$\frac{x^2}{a^2+s} + \frac{y^2}{b^2+s} + \frac{z^2}{c^2+s} = 1$$

Interpreting s as the unknown, this equation is a cubic and the Algebra's main theorem grants three solutions, that are traditionally called (ξ, η, ζ). These roots are the requested Mathieu coordinates of the point (x, y, z); those coordinates can be visualized noting that the surface with ξ constant is an ellipsoid, while those obtained by setting η or ζ constant are hyperboloids. In Figure C.2 are sketched those coordinates in 2D: the ellipses are curves with ξ constant, while the hyperbolas are those with η constant. For later use, here are the Cartesian coordinates expressed in (ξ, η, ζ):

$$\begin{aligned} x &= \pm\Big(\frac{(\xi+a^2)(\eta+a^2)(\zeta+a^2)}{(b^2-a^2)(c^2-a^2)}\Big)^{\frac{1}{2}} \\ y &= \pm\Big(\frac{(\xi+b^2)(\eta+b^2)(\zeta+b^2)}{(c^2-b^2)(a^2-b^2)}\Big)^{\frac{1}{2}} \\ z &= \pm\Big(\frac{(\xi+c^2)(\eta+c^2)(\zeta+c^2)}{(a^2-c^2)(b^2-c^2)}\Big)^{\frac{1}{2}} \end{aligned} \tag{C.1}$$

To be useful in electromagnetism, we need to know the Laplacian in those new coordinates; by defining a convenient coefficient

$$R_u = \sqrt{(a^2+u)(b^2+u)(c^2+u)} \quad (u = \xi,\, \eta,\, \zeta)$$

And with a fair amount of algebra, the Laplacian can be written in a way that should be acceptable for the youths of 2000:

$$\nabla^2\phi = \frac{4}{(\xi-\eta)(\zeta-\xi)(\eta-\zeta)}\Big((\eta-\zeta)R_\xi\frac{\partial}{\partial\xi}\big(R_\xi\frac{\partial\phi}{\partial\xi}\big) + (\zeta-\xi)R_\eta\frac{\partial}{\partial\eta}\big(R_\zeta\frac{\partial\phi}{\partial\eta}\big) + (\xi-\eta)R_\zeta\frac{\partial}{\partial\zeta}\big(R_\zeta\frac{\partial\phi}{\partial\zeta}\big)\Big) \quad \text{(C.2)}$$

The general solutions for $\nabla^2\phi = 0$ in those coordinates are called *ellipsoidal harmonics*. Our setup is however quite simple and all will be needed is the separation of the coordinate variables.

Now, we are using those uncomfortable coordinates because a great gain is expected, and here it is: the coordinate ξ was said to have ellipsoids as iso-surfaces; it is what we need to implement the ellipsoidal boundary conditions. Furthermore, the Laplacian obtained has the three variables nicely separated, allowing to treat them independently.

C.2 The solution in a parallel field

An uniform and parallel field, say in direction x and strength H_0, can be seen as the gradient of the scalar potential $\phi_0 = -H_0 x$. In our curvaceous coordinates, by use of C.1 the potential reads:

$$\phi_0 = -H_0 x = -H_0 Big(\frac{(\xi+a^2)(\eta+a^2)(\zeta+a^2)}{(b^2-a^2)(c^2-a^2)}\Big)^{\frac{1}{2}}$$

It is a solution of Laplace equation, and the three coordinates are conveniently separated; this separation can be highlighted

$$\phi_0 = C_1 F_1(\xi) F_2(\eta) F_3(\zeta)$$

Is now time to insert our ellipsoid, and is reasonable to hope that it will bring an ellipsoidal perturbation to the previous potential. Betting on that, [1, §3.25] a will-be solution can be written as

$$\phi_1 = C_2 G_1(\xi) F_2(\eta) F_3(\zeta)$$

In this will-be solution $F_2(\eta)$ and $F_3(\zeta)$ are known, from the parallel field potential. Remains to get the new $G_1(\xi)$, that has to be dropped into the Laplace equation; and thanks to the fact that C.2 is quite nice, the result sorts out also reasonably clean:

$$R_\xi\frac{d}{d\xi}\Big(R_\xi\frac{dG_1}{d\xi}\Big) - \Big(\frac{b^2+c^2}{4} + \frac{\xi}{4}\Big) = 0 \quad \text{(C.3)}$$

This second-order differential equation, with only one variable, can finally be solved, at least as integral.

Exploiting the fact that a solution ϕ_0 is already known, will get:

$$G_1(\xi) = F_1(\xi) \int \frac{\mathrm{d}\chi}{F_1^2(\xi) R_\xi}$$

So our perturbation due to the ellipsoid can be written in term of the parallel field potential:

$$\phi_1(\xi, \eta, \zeta) = \phi_0 \frac{C_2}{C_1} \int_\xi^\infty \frac{\mathrm{d}\xi'}{F_1^2(\xi') R_{\xi'}} \tag{C.4}$$

This result is what was needed: a solution of Laplace equation that can accept ellipsoidal boundary conditions. It contain a nasty integral, that it will be sorted out only at the end. This solution (combined with the trivial one of the parallel field) contains all what is needed to describe an ellipsoid, but still a bit too generic: it must be properly tuned to represent our paramagnetic ellipsoid.

C.3 Paramagnets

At first, is useful to make a consideration of convenience: for the current purposes only the field *inside* the ellipsoid is relevant for the study [1], so is possible to disregard the clumsy computation of the field outside and concentrate only on the easy inside.

In the (ξ, η, ζ) coordinates, $\xi > 0$ means outside and $\xi < 0$ means inside the ellipsoid; now, the function $G_1(\xi)$ just founded with hard work is not defined for $\xi = -a^2$, thus inside the ellipsoid it can't be used and the potential must assume only the simple form

$$\phi^- = C_3 F_1(\xi) F_2(\eta) F_3(\zeta) = \frac{C_3}{C_1} \phi_0 = C_4 * H_0 x$$

That is, a parallel field of different strength. Now, is time to set the permeability of the ellipsoid at μ_1 and at μ_2 for the surrounding medium [2]; and with some hidden calculations is possible to get the constant of proportionality, while coming back to Cartesian coordinates:

$$\phi^- = -\frac{H_0 x}{1 + \frac{N_a}{2\mu_2}(\mu_1 - \mu_2)} \tag{C.5}$$

While the annoying elliptic integral inherited from C.4 has been hidden in the *geometric* constant N_a [3, §4]:

$$N_a = v \int_{\xi=0}^\infty \frac{\mathrm{d}\xi'}{F_1^2(\xi') R_{\xi'}} = \frac{abc}{2} \int_0^\infty \frac{\mathrm{d}s}{(s + a^2)^{\frac{3}{2}} (s + b^2)^{\frac{1}{2}} (s + c^2)^{\frac{1}{2}}}$$

The incredibly simple equation C.5 is all that is needed, and its linearity and cleanliness explain why the ellipsoidal model is so widely used, although was pretty hard to solve.

But is not over! The analysis has been carried only for a field parallel to the x axis, that happened to

[1] unless particle-particle interaction should be taken into account, with an accuracy greater than a dipole approximation
[2] Permeabilities that are supposed constant and isotropic

Table C.1: Representative values of the N_i

Ellipsoid shape	a	b	c	N_a	N_b	N_c	Image
Needle	1	0	0	0	0.5	0.5	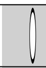
Long potato	2	1	1	0.18	0.41	0.41	
Sphere	1	1	1	0.33	0.33	0.33	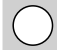
Flat potato	1	2	2	0.52	0.24	0.24	
Disk	0	1	1	1	0	0	

be parallel also to the a axis of the ellipsoid. Luckily, electromagnetism is linear and so, for a parallel field in a generic direction $\mathbf{H}_0 = (H_{0x}, H_{0y}, H_{0z})$, with scalar potential $\phi(x, y, z) = -H_{0x}x - H_{0y}y - H_{0z}z$, the potential inside the Cartesian-oriented ellipsoid is just the sum of the three components:

$$\phi^-(x,y,z) = -\frac{H_{0x}x}{1+\frac{N_a}{\mu_2}(\mu_1-\mu_2)} - \frac{H_{0y}y}{1+\frac{N_b}{\mu_2}(\mu_1-\mu_2)} - \frac{H_{0z}z}{1+\frac{N_c}{\mu_2}(\mu_1-\mu_2)} \tag{C.6}$$

C.3.1 The integral

The general solution of the integral for N_a is not analytically well manageable; it is however reasonable to simplify the ellipsoid to a spheroid, that is an ellipsoid with two axes equal (or can be seen as a sphere that has been pulled or squeezed only in one direction). This simplification is believed to preserve the key features of the physics to be modelled. Why do that? Because it happens that with $b = c$ the integral become much more solvable, and in the following, the orientation of the ellipsoid with respect to the external field can be expressed with just one angle, instead of the two needed for the generic ellipsoid. With some help from the algebraic software `Mathematica`, the integral is solved, here for the case when ab:

$$\begin{aligned} N_a &= v\int_{\xi=0}^{\infty}\frac{\mathrm{d}\xi'}{F_1^2(\xi')R_{\xi'}} = \frac{abc}{2}\int_0^{\infty}\frac{\mathrm{d}s}{(s+a^2)^{\frac{3}{2}}(s+b^2)^{\frac{1}{2}}(s+c^2)^{\frac{1}{2}}} \\ &= \frac{ab^2}{2}\int_0^{\infty}\frac{\mathrm{d}s}{(s+a^2)^{\frac{3}{2}}(s+b^2)} && (b=c) \\ &= \frac{b^2}{b^2-a^2} + \frac{b^2 a\cosh^{-1}(a/b)}{(a^2-b^2)^{3/2}} && (a>b) \end{aligned} \tag{C.7}$$

This result doesn't look so bad; it is possible to rewrite it in terms of aspect ratio or eccentricity of the ellipsoid. Is enough here to observe that N_a is a purely geometric factor, depending only on the aspect-ratio; should be noted also that and the sum of the three is unity: $N_a + N_b + N_c = 1$, and in the case of the spheroid, only one value is needed, since $N_b = N_c$, thus $Na = 1 - N_b - N_c = 1 - 2N_b$. It is useful to tabulate its values for some representative shapes; see [53, 54] for more values and a proper derivation.

.

C.4 Practical Results

It is now the point to harvest the fruits of the mathematical challenge; at first is convenient to deploy the rotational symmetry of the spheroid just introduced so to simplify the geometric setup: a single angle θ can be used to express the orientation of the ellipsoid with respect to the field, figure C.3.

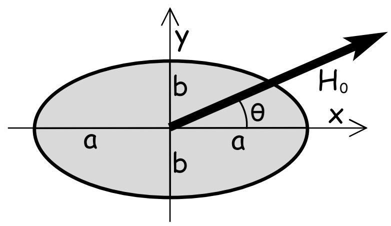

Figure C.3: Profile of the spheroid and its orientation with respect to the external field. Here the hidden semiaxis c is equal to the b. [111]

As the figure implicitly suggests, in this properly simplified (but general) setup, the ellipsoid defines again the cartesian axes, while the external field is tilted at an angle θ, $\mathbf{H}_0 = (\cos\theta H_0, \sin\theta H_0, 0)$.

C.4.1 Field

Adapting equation (C.6) to this setup, the potential inside the ellipsoid reads:

$$\phi^-(x,y,z) = -\frac{\cos\theta H_0 x}{1+\frac{N_a}{\mu_2}(\mu_1-\mu_2)} - \frac{\sin\theta H_0 y}{1+\frac{N_b}{\mu_2}(\mu_1-\mu_2)} \tag{C.8}$$

And by taking the gradient is possible to get the corresponding field

$$\begin{aligned} H_x^- &= H_0\frac{\cos\theta}{1+\frac{N_a}{\mu_2}(\mu_1-\mu_2)} \\ H_y^- &= H_0\frac{\sin\theta}{1+\frac{N_b}{\mu_2}(\mu_1-\mu_2)} \\ H_z^- &= 0 \end{aligned} \tag{C.9}$$

As was anticipated, the field inside is no more parallel to the imposed one, unless $N_a = N_b$ (a sphere, and rotational invariance of the sphere guarantees that the field must be parallel to the external one) or when $\mu_1 = \mu_2$, meaning the ellipsoid has same susceptibility of the medium, and nothing should happen. A convenient way to represent this result is to introduce the *demagnetizing factors* L_{ij} defined by the equation:

$$H_x^- = H_0 - L_{11}\frac{1}{\mu_2}P_{1x} \tag{C.10}$$

And setting the magnetization vector $\mathbf{P}$ as

$$\frac{1}{\mu_0}\mathbf{P_1} = (\mu_1 - \mu_0)\mathbf{H}_0 = \chi\mathbf{P} \tag{C.11}$$

Leading to the demagnetizing components to be simply the beloved elliptic integral, multiplied by a ratio of the susceptibilities:

$$\begin{aligned} L_{11} &= N_a\frac{\mu_1 - \mu_2}{\mu_1 - \mu_0} = N_a\frac{\chi_1 - \chi_2}{\chi_1} \\ L_{22} &= N_b\frac{\mu_1 - \mu_2}{\mu_1 - \mu_0} = N_a\frac{\chi_1 - \chi_2}{\chi_1} \\ L_{33} &= N_c\frac{\mu_1 - \mu_2}{\mu_1 - \mu_0} = N_a\frac{\chi_1 - \chi_2}{\chi_1} \end{aligned} \tag{C.12}$$

The indexes used anticipate that they are the components of the demagnetizing tensor $\mathbf{L}_{ij}$(diagonal, thanks to the alignment of the ellipsoid with the axes)[3], that relate the external field to the magnetization (the $\frac{1}{\mu_0}$ outside deviates from the official definition, so to get the $\mathbf{L}$ completely a-dimensional):

$$\mathbf{H}^- = \mathbf{H_0} + \mathbf{L}\frac{1}{\mu_0}\mathbf{P} = \mathbf{H_0} + \mathbf{M} \tag{C.13}$$

The magnetization represent the local magnetic field that the material set up in response of the magnetic field, and the demagnetizing tensor represent how much this deviate from the plain paramagnet outside of the ellipsoid.

C.4.2 Energy

The field is now determined; the next step is to calculate the energy. The definition of magnetostatic energy is not straightforward; taking a leap of faith, say that the energy is an integral over the volume [33], [1]:

$$U_r = -\frac{1}{2}\int \mu_1\mathbf{H}\cdot\mathbf{H}_0\,\mathrm{d}v$$

Where $\mathbf{H}$ is the external magnetic field, and $\mathbf{H}_0$ the modified field; μ_1, $\mu 2$ are the permeabilities of the ellipsoid and of the medium. The field as from equation (C.9) is constant inside the ellipsoid, thus the integral can be easily sorted out as the volume $V = \frac{4}{3}\pi abc$ of the ellipsoid:

[3] There are good reason to believe, but I didn't manage to prove, that any kind of potato will give rise to a diagonalizable tensor. If that is true, the ellipsoid is an excellent model, since its three independent components (3 the N_i, -1 the condition $N_a + N_b + N_c = 1$, and +1 again from the scaling) can serve as basis. But maybe the diagonalizability doesn't hold for weird shapes, like an helix that doesn't respect chiral symmetry. The relevance of that issue for the oil industry is dubious, $\geq$ but further work will be deserved to it.

$$\begin{aligned}
U_r &= -\frac{1}{2}\int_V (\mu_2-\mu_1)\mathbf{H}\cdot\mathbf{H}_0 \,\mathrm{d}v = \frac{1}{2}V(\mu_2-\mu_1)\mathbf{H}\cdot\mathbf{H}_0 \\
&= -\frac{V}{2}\mu_1\Big(H_0^2\frac{\cos^2\theta}{1+\frac{N_a}{\mu_2}(\mu_1-\mu_2)} - \frac{\sin^2\theta}{1+\frac{N_b}{\mu_2}(\mu_1-\mu_2)}\Big) \\
&= \frac{V}{2}\mu_1 H_0^2\Big(\cos^2\theta\frac{\frac{(\mu_1-\mu_2)}{\mu_2}(N_a-N_b)}{\big(1+\frac{N_a}{\mu_2}(\mu_1-\mu_2)\big)\big(1+\frac{N_b}{\mu_2}(\mu_1-\mu_2)\big)} + \frac{1}{1+\frac{N_b}{\mu_2}(\mu_1-\mu_2)}\Big)
\end{aligned}$$

Now, since we are interested in the dependence of the energy on the angle, in the last expression the constant term could be dropped, leaving with

$$U_r = \frac{V}{2}\frac{\mu_1(\mu_1-\mu_2)}{\mu_2}H_0^2\cos^2\theta\frac{N_a-N_b}{\big(1+\frac{N_a}{\mu_2}(\mu_1-\mu_2)\big)\big(1+\frac{N_b}{\mu_2}(\mu_1-\mu_2)\big)} \tag{C.14}$$

This expression is (almost) the final result of the ellipsoid calculation. In it, appears the volume V of the particle; the square H_0^2 of the external field; a combination of the susceptibilities; a number representing the shape of the ellipsoid; and finally, most important, the $\cos^2\theta$ component, that represent the variation of the energy with the ellipsoid alignment. In honour of this primary importance, and to improve readability, let's conceal all the other dependencies into a clean k factor:

$$U_r = k\,\cos^2\theta \tag{C.15}$$

Compare this result with the energy of a dipole, that goes like $\alpha\cos\theta$. The sign of k decide if the ellipsoid prefer to align the axis a along or perpendicular to the field: for a long potato with high permeability $\{\mu_1>\mu_2,\, a>b\} \Rightarrow k<0$ and will align along the field; for a flat potato of the same material, $\{\mu_1>\mu_2,\, a<b\} \Rightarrow k>0$ will set the (short) a axis perpendicular to the field. For a material with lower permeability, the opposite holds.

For most practical purposes the permeability of the medium could be considered the same as for vacuum, μ_0, while the suspended ellipsoid has a strong susceptibility $\chi = (\mu_1-\mu_0)/\mu_0$. This is not stricly an approximation, and he full general case can always be revived. With this simplification, the k factor that will be used is:

$$k = \frac{1}{2}V\mu_0\chi(\chi+1)H_0^2\frac{N_a-N_b}{\big(1+N_a\chi\big)\big(1+N_b\chi\big)} \tag{C.16}$$

A further approximation, useful to verify qualitatively the behaviour of our ellipsoid, is to take the limit shape of a needle, with values from table C.1 and consider $|\chi| \ll 1$:

$$k \simeq -\frac{1}{4}V\mu_0\chi H_0^2 \tag{C.17}$$

while for a disk it is:

$$k \simeq \frac{1}{2} V \mu_0 \chi H_0^2 \tag{C.18}$$

To conclude let's see the torque exerted by the field onto the ellipsoid, along the z axis:

$$T_z = -\frac{\partial}{\partial\theta} k \cos^2\theta = 2k\cos\theta\sin\theta = k\sin(2\theta) \tag{C.19}$$

Bibliography

The literature research spanned several fields, so the bibliography is splitted into different topics. Not all articles listed here were cited in the text; are anyway reported as a suggestion for the interested reader.

At first are listed some classic and specialized textbooks, selected for their immediate relevance on the subject, or for the didactic quality as a general introduction.

Second comes the list of the published work that directly relate to the issue of the magnetic mud in drilling. A relevant contribution is brought by Bachelor and Master thesis.

Are then credited the original historical works, usually made around 1900; it was a real fun to hunt the fist scientists that introduced a concept, often with great surprises. Are then collected the recent articles on the mixing formulas, and a selection of good or new articles on the suspended ellipsoids.

The field of Paleomagnetism, specifically when deals with the Depositional Remanent Magnetization, is closely related to the magnetic mud, so many experimental results and techniques can be borrowed from this science. The literature here is abundant and often worth. To close, a colorful ensemble of works from the most disparate fields that were find useful to tackle the magnetic mud subject.

After the bibliograpy, sharing the same numbering with the citations, there is the list of figures present in the report. In the following page, part of the softwares use are credited.

Textbooks

[1] Julius Adams Stratton. *Electromagnetic Theory*. McGraw-Hill book company, inc., 1941. ISBN: 0070621500.

[2] C.J.F. Böttcher. *Theory of Electric Polarisation*. Elsevier Publishing Company, 1952.

[3] Landau, L.D. and Lifšitz, E. M and Pitaevski, L P. *Electrodynamics of Continuous Media*. Pergamon Press, 1984. ISBN: 0750626348.

[4] Landau, L.D. and Lifšitz, E. M and Pitaevski, L P. *Statistical Physics I*. Pergamon Press, 1984.

[5] Frederick Reif. *Fundamentals of statistical and thermal physics*. Auckland: McGraw-Hill, 1985. ISBN: 070518009.

[6] H.A. Barnes, J.F. Hutton, and K. Walters. *An Introduction to Rheology*. Annals of Discrete Mathematics. Elsevier, 1989. ISBN: 9780444871404.

[7] Robert F. Butler. *Paleomagnetism: Magnetic Domains to Geologic Terranes*. Blackwell Scientific Publications, 1992. ISBN: 9780865420700. URL: http://www.earth.ox.ac.uk/research/groups/magnetism/online_resources/paleomagnetism_e-book.

[8] Franz Mandl. *Statistical Physics (3rd Edition)*. Manchester: Wiley, 1997. ISBN: 9780471915324.

[9] J.D. Jackson. *Classical Electrodynamics*. Wiley, 1998. ISBN: 9780471309321.

[10] A.H. Sihvola and Institution of Electrical Engineers. *Electromagnetic Mixing Formulas and Applications*. IEE Publication Series. Institution of Electrical Engineers, 1999. ISBN: 9780852967720.

[11] G. K. Batchelor. *An Introduction to Fluid Dynamics*. Cambridge University Press, Feb. 28, 2000. 662 pp. ISBN: 9780521663960.

[12] John Gregory. *Particles in Water: Properties and Processes*. CRC Press, Sept. 6, 2005. ISBN: 9780203508459.

[13] D. Halliday, R. Resnick, and J. Walker. *Fundamentals of Physics*. John Wiley & Sons, 2010. ISBN: 9780470469118.

[14] R. Caenn, H.C.H. Darley, and G.R. Gray. *Composition and Properties of Drilling and Completion Fluids*. Gulf Professional Pub., 2011. ISBN: 9780123838582.

[15] William T. Coffey. *Langevin Equation: With Applications To Stochastic Problems In Physics, Chemistry and Electrical Engineering (3rd Edition)*. Singapore: World Scientific Publishing Company, 2012. ISBN: 9789814355674.

Directly related works

[16] Hugh S. Williamson and others. "Accuracy prediction for directional measurement while drilling". In: *SPE Drilling & Completion, SPE-67616-PA* 15.4 (2000), pp. 221–233.

[17] A. Saasen et al. "Ilmenite as Weight Material in Water Based and Oil Based Drilling Fluids". In: Society of Petroleum Engineers, SPE-71401-MS, 2001. DOI: doi:10.2118/71401-MS.

[18] Harry Wilson and Andrew G. Brooks. "Wellbore Position Errors Caused by Drilling-Fluid Contamination". In: *SPE Drilling & Completion,SPE-75329-PA* 16.4 (Dec. 1, 2001), pp. 208–213. DOI: 10.2118/75329-PA.

[19] Torgeir Torkildsen et al. "Drilling Fluid affects MWD Magnetic Azimuth and Wellbore Position". In: Society of Petroleum Engineers, SPE-87169-MS, 2004. DOI: 10.2118/87169-MS.

[20] Per A. Amundsen, Torgeir Torkildsen, and Arild Saasen. "Shielding of Directional Magnetic Sensor Readings in a Measurement While Drilling Tool for Oil Well Positioning". In: *Journal of Energy Resources Technology* 128.4 (Oct. 27, 2005), pp. 343–345. DOI: 10.1115/1.2358151.

[21] Timothy Allen. "A quick method to help identify magnetic mud with MWD". In: *ISCWSA meeting, Sperry Drilling - Halliburton* (2009). URL: http://www.iscwsa.net/index.php/download_file/view/20/75/.

[22] Kirsten Marie Leiros. "Termisk fluktuasjon i boreveske". Bacheloroppgave. Stavanger, Norway: UiS, 2009.

[23] Richard Ochoa Hidalgo. "Magnetisk skjerming i borevæske". Bacheloroppgave. Stavanger, Norway: UiS, 2009.

[24] American Petroleum Institute. *API 13A - Purchasing guidelines for drilling mud materials.* 2010.

[25] Per A. Amundsen et al. "SPE-113206-PA Magnetic Shielding During MWD Azimuth Measurements and Wellbore Positioning". In: *SPE Drilling & Completion* 25.2 (2010), pp. 219–222. DOI: http://dx.doi.org/10.2118/113206-pa.

[26] S. Ding et al. "Experimental Investigation of the Magnetic Shielding Effect of Mineral Powders in a Drilling Fluid". In: *Particulate Science and Technology* 28.1 (Jan. 26, 2010), pp. 86–94. DOI: 10.1080/02726350903500781.

[27] Øystein Viken. "Magnetisering av ellipsoider i et ytre felt". Bacheloroppgave. Stavanger, Norway: UiS, 2010.

[28] Kristoffer Tellefsen. "Effect of Drilling Fluid Content on Directional Drilling: Shielding of Directional Magnetic Sensor in MWD Tools". Masteroppgave. Stavanger, Norway: UiS, 2011.

[29] ICSWsA Committee. "Introduction to wellbore positioning". In: *University of the Highlands and Islands* (2012). URL: http://www.iscwsa.net/.

[30] Kristoffer Tellefsen et al. "The Effect of Drilling Fluid Content on Magnetic Shielding of Downhole Compasses in MWDs". In: Society of Petroleum Engineers, SPE 150548-MS, 2012. DOI: 10.2118/150548-MS.

[31] Tor Inge Waag et al. "The design of BHA and the placement of magnetometer sensors influence how magnetic azimuth is distorted by the magnetic properties of drilling fluids". In: *SPE Drilling & Completion, SPE-151039-PA* 27.3 (2012), pp. 393–406.

[32] Zhuo Li. "Paramagnetism Shielding in Drilling Fluid". Masteroppgave. Stavanger, Norway: UiS, 2013.

[33] Per Amund Amundsen. "Notes on magnetic shielding". Stavanger, Norway: UiS, 2014.

[34] Arild Saasen et al. "The shielding effect of drilling fluids on mwd downhole compasses: the effect of drilling fluid composition, contaminants and rheology". In: *ASME 2014 33rd International Conference on Ocean, Offshore and Arctic Engineering*. American Society of Mechanical Engineers, 2014.

[35] L.L. Yan et al. "Study on Erosive and Magnetic Effects of Weighting Agent in a High Density Water-Based Drilling Fluid". In: Print. Offshore Technology Conference, 2014. DOI: 10.4043/24787-MS. (Visited on 04/14/2015).

[36] Steve Grindrod. "Magnetic Mud". In: *41th ISCWSA meeting* (Mar. 21, 2015). URL: http://www.iscwsa.net/index.php/iscwsa-test1/ (visited on 04/14/2015).

Historical works

[37] Ottaviano Fabrizio Mossotti. “Discussione analitica sull’influenza che l’azione di un mezzo dielettrico ha sulla distribuzione dell’elettricità alla superficie di più corpi elettrici disseminati in esso”. In: *Memorie di Mathematica e di Fisica della Società Italiana della Scienza Residente in Modena* 24 (1850), pp. 49–74.

[38] Rudolf Clausius. “Abhandlungen über die mechanische Wärmetheorie”. In: *Friedrich Vieweg und Sohn, Braunschweig* 2 (1867), p. 143.

[39] Émile Mathieu. “Mémoire sur le mouvement vibratoire d’une membrane de forme elliptique”. In: *Journal de mathematique pure et applieé* 13 (1868), pp. 137–203.

[40] J. C. Maxwell Garnett. “Colours in Metal Glasses and in Metallic Films”. In: *Philosophical Transactions of the Royal Society of London A: Mathematical, Physical and Engineering Sciences* 203.359-371 (1904), pp. 385–420. DOI: 10.1098/rsta.1904.0024.

[41] Albert Einstein. “Über die von der molekularkinetischen Theorie der Wärme geforderte Bewegung von in ruhenden Flüssigkeiten suspendierten Teilchen, - English: On the movement of small particles suspended in a stationary liquid demanded by the molecular-kinetic theory of heat”. In: *Annalen der Physik* 322(8) (1905), pp. 549–560.

[42] Paul Langevin. “Magnétisme et théorie des électrons”. In: *Annales de la chimie et de la physique* SER 8 (T5 1905), p. 70.

[43] Peter Josef William Debye. *Polar Molecules.* New York: Literary Licensing, LLC, 1929. 174 pp. ISBN: 9781258453916.

[44] Francis Perrin. “Mouvement brownien d’un ellipsoide - I. Dispersion diélectrique pour des molécules ellipsoidales”. In: *J. Phys. Radium* 5.10 (1934), pp. 497–511. DOI: 10.1051/jphysrad:01934005010049700.

[45] Lars Onsager. “Electric Moments of Molecules in Liquids”. In: *Journal of the American Chemical Society* 58.8 (Aug. 1, 1936), pp. 1486–1493. DOI: 10.1021/ja01299a050.

Effective Susceptibility of a mixture

[46] Z. Hashin and S. Shtrikman. "A Variational Approach to the Theory of the Effective Magnetic Permeability of Multiphase Materials". In: *Journal of Applied Physics* 33.10 (1962), pp. 3125–3131. DOI: 10.1063/1.1728579.

[47] B. U. Felderhof, G. W. Ford, and E. G. D. Cohen. "Cluster expansion for the dielectric constant of a polarizable suspension". In: *Journal of Statistical Physics* 28.1 (1982), pp. 135–164.

[48] Ari H. Sihvola and Jin Au Kong. "Effective permittivity of dielectric mixtures". In: *Geoscience and Remote Sensing, IEEE Transactions on* 26.4 (1988). Print, pp. 420–429.

[49] Kimmo Kalervo Kärkkäinen, Ari Henrik Sihvola, and Keijo I. Nikoskinen. "Effective Permittivity of Mixtures: Numerical Validation by the FDTD Methodical problems". In: *IEEE TRANSACTIONS ON GEOSCIENCE AND REMOTE SENSING*. International Conference on Magnetism (Part II) 38 (2000), pp. 1455–1456.

[50] Stefano Giordano. "Effective medium theory for dispersions of dielectric ellipsoids". In: *Journal of Electrostatics* 58.1 (May 2003), pp. 59–76. DOI: 10.1016/S0304-3886(02)00199-7.

[51] Ari Sihvola. "Dielectric Polarization and Particle Shape Effects". In: *Journal of Nanomaterials* 2007 (2007), pp. 1–9. ISSN: 1687-4110. DOI: 10.1155/2007/45090.

[52] Moran Wang and Ning Pan. "Predictions of effective physical properties of complex multiphase materials". In: *Materials Science and Engineering: R: Reports* 63.1 (Dec. 20, 2008), pp. 1–30. DOI: 10.1016/j.mser.2008.07.001.

The Ellipsoid in suspension

[53] Edmund C. Stoner Sc D. F.R.S. "The demagnetizing factors for ellipsoids". In: *The London, Edinburgh, and Dublin Philosophical Magazine and Journal of Science* 36.263 (Dec. 1, 1945), pp. 803–821. ISSN: 1941-5982. DOI: 10.1080/14786444508521510.

[54] J. A. Osborn. "Demagnetizing Factors of the General Ellipsoid". In: *Phys. Rev.* 67 (11-12 1945), pp. 351–357. DOI: 10.1103/PhysRev.67.351.

[55] Seymour H. Koenig. "Brownian motion of an ellipsoid. A correction to Perrin's results". In: *Biopolymers* 14.11 (Nov. 1, 1975), pp. 2421–2423. DOI: 10.1002/bip.1975.360141115.

[56] A. D. Shine and R. C. Armstrong. "Experimental studies of suspended ferromagnetic fibers in a magnetic field". In: *Rheologica Acta* 26.2 (Mar. 1, 1987), pp. 162–171. DOI: 10.1007/BF01331974.

[57] S. R. Strand and S. Kim. "Dynamics and rheology of a dilute suspension of dipolar nonspherical particles in an external field: Part 1. Steady shear flows". In: *Rheologica acta* 31.1 (1992), pp. 94–117.

[58] Jan Gimsa. "A comprehensive approach to electro-orientation, electrodeformation, dielectrophoresis, and electrorotation of ellipsoidal particles and biological cells". In: *Bioelectrochemistry* 54.1 (2001), pp. 23–31.

[59] Y. Han et al. "Brownian Motion of an Ellipsoid". In: *Science* 314.5799 (Oct. 27, 2006), pp. 626–630. DOI: 10.1126/science.1130146.

[60] J.H. Sánchez and C. Rinaldi. "Magnetoviscosity of dilute suspensions of magnetic ellipsoids obtained through rotational Brownian dynamics simulations". In: *Journal of Colloid and Interface Science* 331.2 (2009), pp. 500–506. DOI: 10.1016/j.jcis.2008.11.061.

[61] I Torres-Díaz and C Rinaldi. "Brownian dynamics simulations of ellipsoidal magnetizable particle suspensions". In: *Journal of Physics D: Applied Physics* 47.23 (June 11, 2014), p. 235003. DOI: 10.1088/0022-3727/47/23/235003.

Paleomagnetism

[62] E. A. Johnson, Thomas Murphy, and O. W. Torreson. "Pre-history of the Earth's magnetic field". In: *Terrestrial Magnetism and Atmospheric Electricity* 53.4 (1948), pp. 349–372. ISSN: 0096-8013. DOI: 10.1029/TE053i004p00349.

[63] R. F. King. "The Remanent Magnetism of Artificially Deposited Sediments". In: *Geophysical Supplements to the Monthly Notices of the Royal Astronomical Society* 7.3 (Dec. 1, 1955), pp. 115–134. DOI: 10.1111/j.1365-246X.1955.tb06558.x.

[64] Peter B. Nozharov. "On the theory of depositional remanent magnetization in sediments: Influence of brownian motion of rotation upon the magnetic orientation of sediments". In: *Pure and applied Geophysics* 67.1 (Dec. 1, 1967), pp. 123–127. DOI: 10.1007/BF00880569.

[65] Frank D. Stacey. "On the role of Brownian motion in the control of detrital remanent magnetization of sediments". In: *pure and applied geophysics* 98.1 (1972), pp. 139–145.

[66] Kenneth L. Verosub. "Depositional and postdepositional processes in the magnetization of sediments". In: *Reviews of Geophysics* 15.2 (1977), pp. 129–143. DOI: 10.1029/RG015i002p00129.

[67] C. E. Barton, M. W. McElhinny, and D. J. Edwards. "Laboratory studies of depositional DRM". In: *Geophysical Journal International* 61.2 (1980), pp. 355–377.

[68] V. P. Shcherbakov and V. V. Shcherbakova. "On the theory of depositional remanent magnetization in sedimentary rocks". In: *Geophysical surveys* 5.4 (Feb. 1, 1983), pp. 369–380. DOI: 10.1007/BF01453987.

[69] Ran Lu, Subir K. Banerjee, and James Marvin. "Effects of clay mineralogy and the electrical conductivity of water on the acquisition of depositional remanent magnetization in sediments". In: *Journal of Geophysical Research: Solid Earth (1978–2012)* 95 (B4 1990), pp. 4531–4538.

[70] Xavier Quidelleur et al. "Field dependence on magnetization of laboratory-redeposited deep-sea sediments: First results". In: *Earth and Planetary Science Letters* 133.3 (July 1995), pp. 311–325. DOI: 10.1016/0012-821X(95)00088-T.

[71] K. Katari, L. Tauxe, and John King. "A reassessment of post-depositional remanent magnetism: preliminary experiments with natural sediments". In: *Earth and Planetary Science Letters* 183.1 (Nov. 30, 2000), pp. 147–160. DOI: 10.1016/S0012-821X(00)00255-7.

[72] Kaushik Katari and Jeremy Bloxham. "Effects of sediment aggregate size on DRM intensity: a new theory". In: *Earth and Planetary Science Letters* 186.1 (Mar. 15, 2001), pp. 113–122. DOI: 10.1016/S0012-821X(00)00386-1.

[73] Brian Carter-Stiglitz, Jean-Pierre Valet, and Maxime LeGoff. "Constraints on the acquisition of remanent magnetization in fine-grained sediments imposed by redeposition experiments". In: *Earth and Planetary Science Letters* 245.1 (May 15, 2006), pp. 427–437. ISSN: 0012-821X. DOI: 10.1016/j.epsl.2006.03.002.

[74] Lisa Tauxe, Jason L. Steindorf, and Andrew Harris. "Depositional remanent magnetization: Toward an improved theoretical and experimental foundation". In: *Earth and Planetary Science Letters* 244.3 (Apr. 30, 2006), pp. 515–529. DOI: 10.1016/j.epsl.2006.02.003.

[75] Ritayan Mitra and Lisa Tauxe. "Full vector model for magnetization in sediments". In: *Earth and Planetary Science Letters* 286.3 (Sept. 2009), pp. 535–545. DOI: 10.1016/j.epsl.2009.07.019.

[76] Valeriy Shcherbakov and Natalia Sycheva. "On the mechanism of formation of depositional remanent magnetization: MECHANISM OF FORMATION OF DRM". In: *Geochemistry, Geophysics, Geosystems* 11.2 (Feb. 2010). DOI: 10.1029/2009GC002830.

[77] Lisa Tauxe et al. *Essentials of Paleomagnetism*. Berkeley: University of California Press, Mar. 19, 2010. ISBN: 9780520260313. URL: http://earthref.org/MAGIC/books/Tauxe/Essentials/.

[78] Kenneth P. Kodama. *Paleomagnetism of sedimentary rocks : process and interpretation*. Wiley-Blackwell, 2012. 157 pp. ISBN: 9781444335026.

[79] Simo Spassov and Jean-Pierre Valet. "Detrital magnetizations from redeposition experiments of different natural sediments". In: *Earth and Planetary Science Letters* 351-352 (Oct. 2012), pp. 147–157. DOI: 10.1016/j.epsl.2012.07.016.

[80] Dario Bilardello. "Understanding DRM acquisition of plates and spheres: a first comparative experimental approach". In: *Geophysical Journal International* (July 18, 2013), ggt240. DOI: 10.1093/gji/ggt240.

[81] D. Heslop, A. P. Roberts, and R. Hawkins. "A statistical simulation of magnetic particle alignment in sediments". In: *Geophysical Journal International* 197.2 (May 1, 2014), pp. 828–837. DOI: 10.1093/gji/ggu038.

Interesting works on other fields

[82] Wikipedia. *Susceptibility*. 1860. URL: https://en.wikipedia.org/wiki/Magnetic_susceptibility.

[83] C. J. M. Wolff. “Borehole Position Uncertainty - Analysis of Measuring Methods and Derivation of Systematic Error Model”. In: *Journal of Petroleum Technology* - 33.12 (1981), pp. 2338–2350. DOI: 10.2118/9223-PA.

[84] William S. Callaway and James L. McAtee. “Magnetic susceptibilities of representative smectites”. In: *American Mineralogist* 70.9 (Oct. 1, 1985), pp. 996–1003.

[85] M. Loewenberg. “Stokes resistance, added mass, and Basset force for arbitrarily oriented, finite-length cylinders”. In: *Physics of Fluids A: Fluid Dynamics (1989-1993)* 5.3 (1993), pp. 765–767.

[86] A. Lazarian. “Davis-Greenstein alignment of non-spherical grains”. In: *The Astrophysical Journal* 453 (Nov. 1995), p. 229. DOI: 10.1086/176382.

[87] C. Tsouris and T. C. Scott. “Flocculation of Paramagnetic Particles in a Magnetic Field”. In: *Journal of Colloid and Interface Science* 171.2 (May 1995), pp. 319–330. DOI: 10.1006/jcis.1995.1186.

[88] Mikael Rasmusson et al. “The Dynamic Mobility and Dielectric Response of Sodium Bentonite”. In: *Journal of Colloid and Interface Science* 189.1 (May 1, 1997), pp. 92–100. DOI: 10.1006/jcis.1997.4793.

[89] Hiroki Chihara, Toshihide Okamura, and Chiaki Uyeda. “The magnetic ordering of graphite grains and its application to astrophysical problems”. In: *Journal of Magnetism and Magnetic Materials*. International Conference on Magnetism (Part II) 177–181, Part 2 (Jan. 1998), pp. 1455–1456. DOI: 10.1016/S0304-8853(97)00878-0.

[90] Sonia Melle et al. “Rotational dynamics in dipolar colloidal suspensions: video microscopy experiments and simulations results”. In: *Journal of Non-Newtonian Fluid Mechanics* 102.2 (Feb. 15, 2002), pp. 135–148. DOI: 10.1016/S0377-0257(01)00174-4.

[91] B. Huke and M. Lücke. “Magnetic properties of colloidal suspensions of interacting magnetic particles”. In: *Reports on Progress in Physics* 67.10 (2004), p. 1731.

[92] Hilmar Koerner et al. "Generating Triaxial Reinforced Epoxy/Montmorillonite Nanocomposites with Uniaxial Magnetic Fields". In: *Chemistry of Materials* 17.8 (Apr. 1, 2005), pp. 1990–1996. DOI: 10.1021/cm048139m.

[93] Joan Connolly et al. "Manipulation of modified clay particles in a nematic solvent by a magnetic field". In: *Journal of Physics: Condensed Matter* 19.15 (Apr. 16, 2007), p. 156103. DOI: 10.1088/0953-8984/19/15/156103.

[94] Kaye & Laby A.E Drake. *Table of magnetic materials*. URL: http://www.kayelaby.npl.co.uk/general_physics/2_6/2_6_6.html.

[95] Wikipedia. *Earth's magnetic field*. URL: https://en.wikipedia.org/wiki/Earth_magnetic_field.

Image sources

[96] Wikimedia Commons. *Face transformations, by Albrecht Dürer*. 1528. URL: http://commons.wikimedia.org/wiki/File:Durer_face_transforms.jpg.

[97] Wikimedia Commons. *The code of Hammurabi, diorite stele, incorporated by the French and now on show at the Louvre*. To actually see the weighted average formula here, some imagination is needed. -1750. URL: http://en.wikipedia.org/wiki/Code_of_Hammurabi#/media/File:Code-de-Hammurabi-1.jpg.

[98] Composed by the author with Inkscape+Photoshop with various old photos. *Some contributors for the mixing formulas*. From left: Ottaviano Mossotti, Rudolf Clausius, Ludvig Lorenz, Hendrik Lorentz, James Clark Maxwell, JWS Raylegh. It must be noted that the Maxwell-Garnett formula was derived by one physicist, apparently with surname Garnett and *name* J C Maxwell, [40], probably in honour of the older colleague, but was impossible to find its portrait. 1900.

[99] Cropped and pasted from the Paleomagnetism textbook [7, §8] figure 8.5(a) pag. 189. *Magnetosome*. 1992.

[100] items at the level of the magnetic mud problems that is less than the total number of physicists on earth. More sub-problems must be generated as was done in this thesis. Drawn by the author with Inkscape. If any of the items illustrated has five sub-items (F.eks. there are five main human needs one of which is energy; energy has five main origins-on which one is oil etc.) that lead to $5^8 \simeq 400.000$. *Multiple zoom*. 2015.

[101] Ding te al. reproduced from [26] and slightly modified. *Dinamic magnetization*. 2015.

[102] Drawn by the author with Inkscape not corresponding to real functions. *Dinamic magnetization - the answer*. 2015.

[103] Drawn by the author with Inkscape from calculated graph. *A very quiet sigmoid with hidden internal divergences*. 2015.

[104] Drawn by the author with Inkscape from calculated graph. *Langevin function*. 2015.

[105] as a simplification of commercial BHA Drawn by the author with Inkscape. *BHA*. 2015.

[106] Drawn by the author with Inkscape. *All the roads lead to the Drilling Mud*. 2015.

[107] Drawn by the author with Inkscape. *Aquariums*. 2015.

[108] Drawn by the author with Inkscape. *Condensers with horizontal and vertical layers*. Maybe the idea of this example is original, or maybe it comes from some interiorized exercise of high school physics. Manufacturing condenser of the second kind looks very challenging, and prone to short-circuits. 2015.

[109] Drawn by the author with Inkscape. *Ellipsoid vs. Potato*. The use of potatoes for defining boundary conditions has been proposed by prof. Paul Papatzacos, UiS, who has also suggested Mathieu as the first to introduce elliptic coordinates. 2015.

[110] Drawn by the author with Inkscape. *Orienting angles for the spheroid*. 2015.

[111] Drawn by the author with Inkscape. *Spheroid, 2D profile*. 2015.

[112] Johnson and Murphy [62] as reported by [66]. Scan from paper copy. *Early redeposition experiment*. 2015.

[113] UiS. *Logo of the Universitet i Stavanger, on the front page*. 2015.

[114] Composed by the author with Inkscape collecting images already in use. *The thesis in three images*. 2015.

[115] Drawn by the author with Inkscape supposedly with realitic proportion: Rig height 100m Well length 2km Reservoir cap 200 m wide. *Directional drilling*. 2015.

Software

A vast array of software and online services were used directly in the making of this project; some of the most relevant are listed here:

- Mozilla Firefox, for web browsing, https://www.mozilla.org;
- LaTeX, scientific typesetting, together with several packages, https://www.ctan.org/;
- Google search engine and apps, www.google.com/;
- ShareLatex, online LaTeXcompiler https://www.sharelatex.com;
- Zotero, bibliography management, https://www.zotero.org/;
- Wikipedia, the modern encyclopedia, https://en.wikipedia.org/;
- Mathematica, the help in algebra, www.wolfram.com/mathematica;
- Inkscape, vectorial drawing, https://inkscape.org;
- Photoshop, images handling, www.photoshop.com;
- Comsol multiphysics, finite elements solver (not finalized, but useful), www.comsol.com;
- Adobe Acrobat, to display this file, https://get.adobe.com/it/reader

And a huge amount of software was used unconsciously or indirectly.

Report typesetted in LaTeX, from original source, with ShareLatex compiler. Structure adapted from a template by Marvin Rausand RAMS-NTNU.

Universitet i Stavanger, Norway, 14 June 2015

■